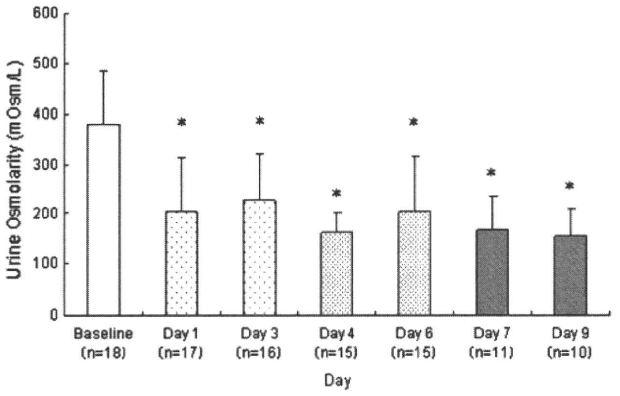

Fig. 2 Urine osmolarity (mean ± SD). Urine osmolarity was measured at 24 h after each dosing (15 mg on days 1 through 3, 30 mg on days 4 through 6, and 60 mg on days 7 through 9). Statistically significant ($*P < 0.05$) decreases in urine osmolarity compared with the baseline were observed at all measurement time points following the start of tolvaptan administration. Urine osmolarity was markedly decreased from the first day of administration at 15 mg, and remained decreased until completion of treatment

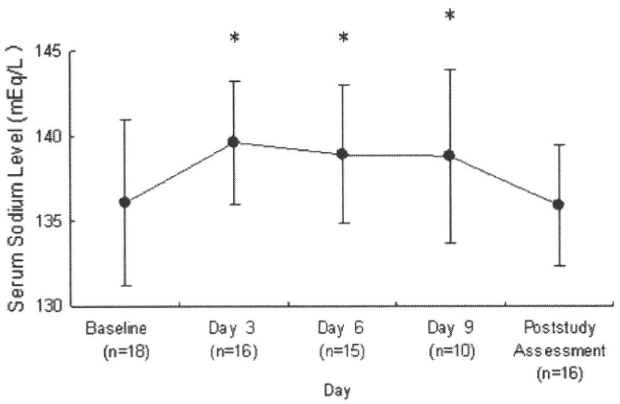

Fig. 3 Serum sodium level (mean ± SD). Serum sodium level was measured at 24 h after the final dosing of 3-day repeated oral administration at each dose (15 mg on days 1 through 3, 30 mg on days 4 through 6, and 60 mg on days 7 through 9). Statistically significant ($*P < 0.05$) increases in serum sodium level compared with the baseline were observed at all measurement time points following the start of tolvaptan administration at 15 mg on day 1. The increased serum sodium level showed a tendency to return to the baseline level after completion of treatment

Efficacy of tolvaptan against intractable ascites and edema

Decreases in body weight and abdominal circumference and improvement of ascites and lower limb edema were observed following administration of tolvaptan beginning from 15 mg. Decreases in mean body weight of 1 kg or more were seen from Day 2 (24 h after first dosing). Changes in body weight following 3-day repeated administration at 15, 30, and 60 mg were, respectively, -1.6 ± 0.9, -2.6 ± 1.2, and -3.4 ± 2.1 kg (mean ± SD),

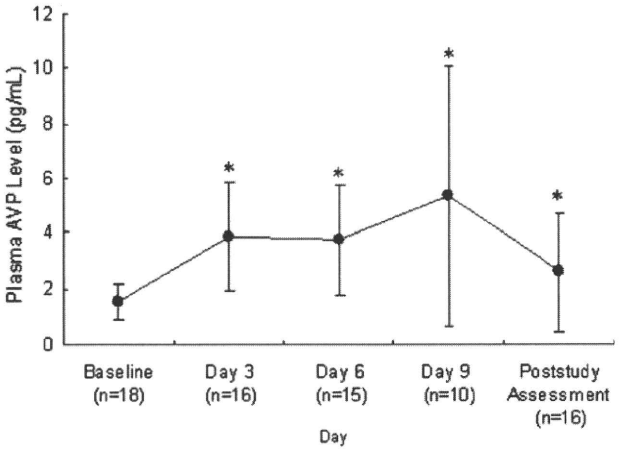

Fig. 4 Plasma AVP level (mean ± SD). Plasma AVP level was measured at 24 h after the final dosing of 3-day repeated oral administration at each dose (15 mg on days 1 through 3, 30 mg on days 4 through 6, and 60 mg on days 7 through 9). Statistically significant ($*P < 0.05$) increases in plasma AVP level compared with the baseline were observed at all measurement time points following the start of tolvaptan administration at 15 mg on day 1. The increased plasma AVP level showed a tendency to return to the baseline level after completion of treatment

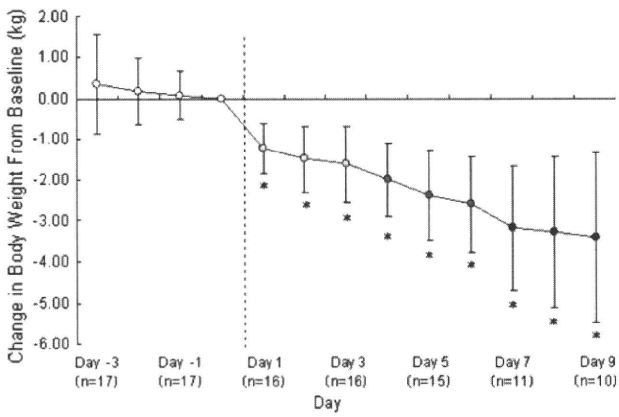

Fig. 5 Change in body weight from baseline (mean ± SD). Body weight was measured at 24 h after each dosing (15 mg on days 1 through 3, 30 mg on days 4 through 6, and 60 mg on days 7 through 9), and changes from the baseline were calculated. Although body weight showed almost no decrease during the pretreatment observation period, statistically significant ($*P < 0.05$) decreases compared with the baseline were observed from the start of tolvaptan administration at 15 mg on day 1. Body weight continued to gradually decrease until the final administration, at which time a statistically significant ($*P < 0.05$) difference from the baseline was observed

and body weight at all postdose measurement time points was significantly decreased compared with the baseline (Fig. 5). As was observed for body weight, decreases in mean abdominal circumference were also observed following tolvaptan administration, with statistically significant differences from the baseline seen at all postdose measurement time points (Fig. 6).

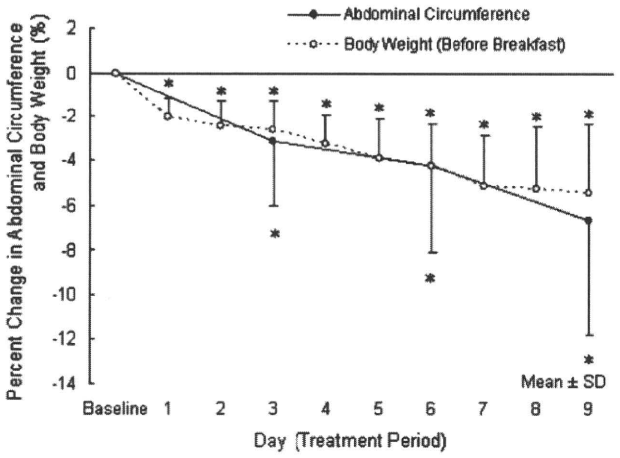

Fig. 6 Time courses of percent change in body weight and abdominal circumference from baseline (mean ± SD). Body weight and abdominal circumference were measured at 24 h after each dosing (15 mg on days 1 through 3, 30 mg on days 4 through 6, and 60 mg on days 7 through 9), and percent change from the baseline was calculated. Both body weight and abdominal circumference showed dose-dependent percent decreases from the baseline with administration of tolvaptan, and statistically significant ($*P < 0.05$) percent decreases from the baseline were observed at all measurement time points

At individual maximum doses, the ascites improvement rate was 87.5% (14 of 16 subjects) and the lower limb edema improvement rate was 83.3% (5 of 6 subjects). The composite ascites/edema improvement rate (primary efficacy endpoint) was 88.2% (15 of 17 subjects) at individual maximum doses or at discontinuation of administration (Table 2a), and 64.7, 80.0, and 90.9%, respectively, after 3-day administration at 15, 30, and 60 mg (Table 2b). In addition, the ascites/edema resolution rate at individual maximum doses was 41.2% (7 of 17 subjects) (Table 3).

Dose–response in this study was evaluated based on the results for changes in cumulative 24-h urine volume, body weight, and abdominal circumference and for improvement of ascites/edema. Regarding body weight, a further body weight decrease of 500 g or more was seen in 8 of 15 subjects following dose titration from 15 to 30 mg/day and in 6 of 11 subjects following dose titration from 30 to 60 mg/day. Decreases in body weight were greater on the first day of administration after dose titration than on the second and third days of administration at the same dose. Regarding abdominal circumference, a further abdominal circumference decrease of 2 cm or more was seen in 7 of 15 subjects following dose titration from 15 to 30 mg/day and in 4 of 11 subjects following dose titration from 30 to 60 mg/day. Of the 7 subjects in whom ascites was not improved (abdominal circumference decrease of less than 2 cm) by 3-day repeated administration at 15 mg/day, 5 subjects showed improvement or resolution of ascites following dose titration to 30 mg/day. Regarding improvement of ascites/edema, although 6 of 17 subjects were assessed as "unchanged" at 15 mg/day, 4 of those 6 subjects showed improvement following dose titration to 30 mg/day. In addition, 2 of 3 subjects assessed as "unchanged" at 30 mg/day showed improvement of ascites/edema following dose titration to 60 mg/day (Fig. 7).

Safety evaluation

Following administration of tolvaptan in a dose-titration manner (15–60 mg/day) to subjects with ascites and/or lower limb edema associated with decompensated liver cirrhosis, adverse events were observed in all 18 subjects who received tolvaptan, for a total of 69 episodes. However, most of the events were considered to have been due either to the pharmacological action of tolvaptan or to the underlying disease. Adverse events observed in 2 or more subjects during the study are summarized in Table 4. Most of the adverse events were observed following administration at 15 mg, and the incidence of adverse events did not increase with dose titration. The most frequently reported adverse events, occurring in 3 subjects or more, were thirst, pollakiuria, insomnia, and increased blood uric acid. No noteworthy changes in clinical laboratory values (hematocrit and hemoglobin), blood pressure, or ECG were observed. In particular, as shown in Table 5, no increases in blood pressure were observed.

Adverse events judged to be adverse drug reactions (i.e., potentially study-related) were also observed in all 18 subjects who received tolvaptan, for a total of 53 episodes. Four serious adverse events (anal fistula, esophageal varices, hepatic neoplasm malignant, and hepatic encephalopathy) were observed in one subject each, and relationship to tolvaptan could not be denied for the anal fistula observed in one subject during 3-day repeated administration at 60 mg. It was confirmed at the poststudy follow-up assessment that all adverse drug reactions were either recovered or ameliorated. Discontinuation of tolvaptan administration or dose reduction was not required in any subject. No adverse events were attributable to aggravation of the underlying disease by administration of tolvaptan in patients with decompensated liver cirrhosis.

Discussion

Although tolvaptan had previously been shown to improve volume expansion in patients with heart failure [11–13] and to raise serum sodium level in cases of hyponatremia [14], its effects on ascites and edema of the extremities

Table 2 Improvement rates at (a) individual maximum doses and (b) each dose

	Grading				Total	Improvement rate (%)[a]	Two-sided 95% CI
	Markedly Improved	Improved	Unchanged	Worsened			
(a)							
Ascites[b]	–	14	2	0	16	87.5	61.7–98.4
Lower limb edema[c]	5	0	1	0	6	83.3	35.9–99.6
Composite ascites/edema[d]	4	11	2	0	17	88.2	63.6–98.5
(b)							
Ascites[b]							
15 mg Day 3	–	9	7	0	16	56.3	
30 mg Day 6	–	12	3	0	15	80.0	
60 mg Day 9	–	10	1	0	11	90.9	
Lower limb edema[c]							
15 mg Day 3	3	0	3	0	6	50.0	
30 mg Day 6	4	1	0	0	5	100.0	
60 mg Day 9	2	0	1	0	3	66.7	
Composite ascites/edema[d]							
15 mg Day 3	1	10	6	0	17	64.7	38.3–85.8
30 mg Day 6	5	7	3	0	15	80.0	51.9–95.7
60 mg Day 9	2	8	1	0	11	90.9	58.7–99.8

[a] Improvement rate = (number of subjects with grading of improved or markedly improved)/(total number of subjects with corresponding symptom) × 100

[b] Grading criteria for ascites: improved = abdominal circumference decreased by 2 cm or more; unchanged = change in abdominal circumference of less than 2 cm; worsened = abdominal circumference increased by 2 cm or more or emergence of ascites

[c] Grading criteria for lower limb edema: markedly improved = resolution or improvement by 2 grades or more; improved = improvement by one grade; unchanged = symptoms unchanged or no symptoms at baseline; worsened = worsened by one grade or more [severity grades: (1) none = no observable pitting; (2) mild = barely visible pitting; (3) moderate = observable pitting; (4) severe = obvious edema at first sight]

[d] Grading criteria for composite ascites/edema: markedly improved = improved for ascites and markedly improved or improved for lower limb edema; improved = unchanged for ascites and markedly improved or improved for lower limb edema; unchanged = unchanged for both ascites and lower limb edema; worsened = worsened for either ascites or lower limb edema

Table 3 Ascites/edema resolution rate at individual maximum doses

Resolved	Not resolved	Total	Resolution rate (%)	Two-sided 95% CI
7	10	17	41.2	18.4–67.1

Ascites/edema resolution rate = (number of subjects resolved)/(total number of subjects) × 100

associated with decompensated liver cirrhosis remained to be explored.

In the present study, we administered tolvaptan as add-on therapy to decompensated liver cirrhosis patients with ascites and/or lower limb edema that was resistant to conventional diuretics. We evaluated efficacy based on changes in body weight, abdominal circumference, daily urine volume, and the severity of lower leg edema, all of which are commonly used parameters for assessing hypervolemia associated with decompensated liver cirrhosis.

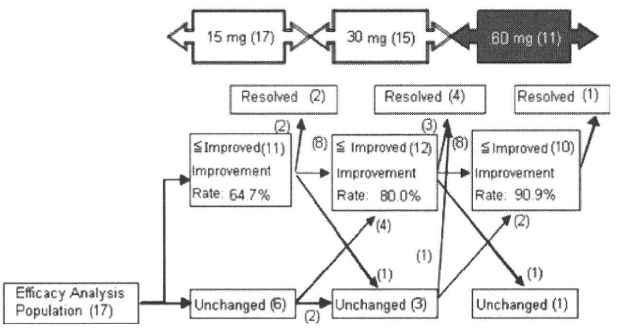

Fig. 7 Changes in composite ascites/edema improvement gradings. Composite ascites/edema improvement was assessed by the investigator after the final dosing of 3-day repeated oral administration at each dose (15 mg on days 1 through 3, 30 mg on days 4 through 6, and 60 mg on days 7 through 9). Four of six subjects assessed as "unchanged" at 15 mg/day were assessed as "improved" or "markedly improved" following dose titration to 30 mg/day, and 2 of 3 subjects assessed as "unchanged" at 30 mg/day were assessed as "improved" or "markedly improved" following dose titration to 60 mg/day, with some subjects showing further improvement with each dose titration. *Numbers in parentheses* indicate number of subjects

Table 4 Summary of adverse events

Item	Tolvaptan 15–60 mg ($N = 18$[a]) n (%)
Adverse events occurring during study (all causes)	18 (100)
Serious adverse events[b]	4 (22.2)
Adverse drug reactions occurring during study	18 (100)
Serious adverse events judged to be adverse drug reactions[c]	1 (5.6)
Adverse events (all causes) by body system and MedDRA preferred term[d]	
Gastrointestinal disorders	
Constipation	2 (11.1)
Esophageal varices	2 (11.1)
General disorders and administration site conditions	
Thirst	15 (83.3)
Malaise	2 (11.1)
Pyrexia	2 (11.1)
Investigations	
Blood uric acid increased	3 (16.7)
Blood glucose increased	2 (11.1)
Metabolism and nutrition disorders	
Anorexia	2 (11.1)
Psychiatric disorders	
Insomnia	4 (22.2)
Renal and urinary disorders	
Pollakiuria	8 (44.4)
Skin and subcutaneous tissue disorders	
Dry skin	2 (11.1)

[a] All subjects who received at least one dose of the study medication (tolvaptan) were included in safety analysis

[b] All-cause serious adverse events occurring during the study were anal fistula, esophageal varices, hepatic neoplasm malignant, and hepatic encephalopathy in one subject each

[c] The only serious adverse event judged to be an adverse drug reaction (i.e., potentially study-related) was anal fistula in one subject

[d] Adverse events occurring in 2 or more subjects are listed

A marked decrease in body weight accompanying increased urine volume was observed soon after the start of administration of tolvaptan, which has a vasopressin V_2 receptor blocking action. Similar to the effects previously seen in patients with heart failure, in the present study administration of tolvaptan also improved ascites and pitting edema (signs indicating hypervolemia) in patients with decompensated liver cirrhosis.

Serum sodium level was also increased following administration of tolvaptan, as was seen in heart-failure patients and cases of hyponatremia. This increase in serum sodium level is considered to be due to an increase in urine volume induced by tolvaptan's vasopressin V_2 receptor antagonist action. As rapid elevation of serum sodium can cause central pontine myelinolysis (CPM), any increase in serum sodium level should not exceed 12 mmol/L within a 24-h period [15, 16]. No complications of CPM or hypernatremia have been observed in clinical studies of tolvaptan.

Although plasma AVP level also increased during administration of tolvaptan, it subsequently decreased after completion of treatment. This increase in plasma AVP was probably due to an increase in plasma osmotic pressure rather than to any decrease in plasma volume, since hematocrit and hemoglobin values remained unchanged after administration of tolvaptan, indicating that a decrease in plasma volume was unlikely. In addition to promoting the reabsorption of water in the kidney via vasopressin V_2 receptors, AVP also induces vasoconstriction via vasopressin V_1 receptors, resulting in an increase in blood pressure. While increased blood pressure can lead to the rupture of esophageal varices, no variceal bleeding was observed in this study, indicating that tolvaptan would be safe for the treatment of hypervolemia as a complication of decompensated liver cirrhosis. Although thirst is a common adverse drug reaction seen with tolvaptan, in the present study thirst was improved by allowing free access to drinking water.

The results of this study demonstrated that tolvaptan exerted a dose-dependent aquaretic effect in patients with furosemide-resistant intractable ascites and/or edema. Most of the adverse events reported were predictable based on tolvaptan's known pharmacological action, and dose titration to 60 mg was well tolerated, with no discontinuations due to adverse events.

In conclusion, based on current study data, tolvaptan is considered to be a safe and effective agent for the treatment of chronic liver failure patients with ascites and/or pitting

Table 5 Blood pressure values

Item (unit)	Time point	*N*	Mean	SD
Systolic blood pressure (mmHg)	Day 1 predose	18	110.5	16.6
	2–4 h postdose	17	108.2	12.4
	6–8 h postdose	18	110.2	12.1
	Day 2	17	109.4	13.7
	Day 3	17	108.9	15.2
	Day 4 predose	17	107.3	16.0
	2–4 h postdose	15	109.1	13.9
	6–8 h postdose	16	105.0	15.9
	Day 5	15	109.5	12.7
	Day 6	15	106.7	12.3
	Day 7 predose	15	108.3	14.2
	2–4 h postdose	11	106.6	10.0
	6–8 h postdose	11	105.5	8.2
	Day 8	11	104.8	11.1
	Day 9	11	104.7	14.6
	Day 10	10	105.8	12.1
Diastolic blood pressure (mmHg)	Day 1 predose	18	68.1	7.6
	2–4 h postdose	17	65.3	9.5
	6–8 h postdose	18	67.0	7.3
	Day 2	17	66.4	7.9
	Day 3	17	67.4	4.7
	Day 4 predose	17	68.1	13.0
	2–4 h postdose	15	65.3	9.0
	6–8 h postdose	16	65.6	9.7
	Day 5	15	68.2	8.7
	Day 6	15	67.1	8.1
	Day 7 predose	15	68.4	9.2
	2–4 h postdose	11	69.3	10.5
	6–8 h postdose	11	69.9	6.7
	Day 8	11	66.4	8.9
	Day 9	11	63.4	4.9
	Day 10	10	68.6	5.9

edema that is resistant to powerful diuretics such as furosemide. We also concluded that continued investigation in a parallel-group comparison study is needed to further clarify the drug's efficacy.

Acknowledgments The authors are most grateful to their fellow researchers and hospitals for their contribution to data collection.

References

1. Guyton AC, Hall JE. Textbook of medical physiology. 10th ed. Philadelphia, PA: WB Saunders Company; 2000. p. 855–6.
2. Yamamura Y, Nakamura S, Itoh S, Hirano T, Onogawa T, Yamashita T, et al. OPC-41061, a highly potent human vasopressin V2-receptor antagonist: pharmacological profile and aquaretic effect by single and multiple oral dosing in rats. J Pharmacol Exp Ther. 1998;287(3):860–7.
3. Doggrell SA. Tolvaptan (Otsuka). Curr Opin Investig Drugs. 2004;5:977–83.
4. Costello-Boerrigter LC, Smith WB, Boerrigter G, Ouyang J, Zimmer CA, Orlandi C, et al. Vasopressin-2-receptor antagonism augments water excretion without changes in renal hemodynamics or sodium and potassium excretion in human heart failure. Am J Physiol Renal Physiol. 2006;290:273–8.
5. Lieberman FL, Ito S, Reynolds TB. Effective plasma volume in cirrhosis with ascites. Evidence that a decreased value does not account for renal sodium retention, a spontaneous reduction in glomerular filtration rate (GFR), a fall in GFR during drug-induced diuresis. J Clin Invest. 1969;48(6):975–81.
6. Lieberman FL, Denison EK, Reynolds TB. The relationship of plasma volume, portal hypertension, ascites, and renal sodium retention in cirrhosis: the "overflow" theory of ascites formation. Ann NY Acad Sci. 1970;170:202–6.
7. Levy M. Pathophysiology of ascites formation. In: Epstein M, editor. The kidney in liver disease. 2nd ed. New York: Elsevier, 1982. p. 245–80.
8. Schrier RW, Arroyo V, Bernardi M, Epstein M, Henriksen JH, Rodes J. Peripheral arterial vasodilation hypothesis: a proposal for the initiation of renal sodium and water retention in cirrhosis. Hepatology. 1988;8(5):1151–7.
9. Shoaf SE, Bramer SL, Bricmont P, Zimmer CA. Pharmacokinetic and pharmacodynamic interaction between tolvaptan, a non-peptide AVP antagonist, furosemide or hydrochlorothiazide. J Cardiovasc Phamacol. 2007;50(2):213–22.
10. Inuyama Symposium Kirokukannkoukai, editors. Proceedings of the 12th Inuyama Symposium: hepatitis A and fulminant hepatitis (in Japanese). Tokyo: Chugai Igakusha; 1982. p. 124.
11. Gheorghiade M, Niazi I, Ouyang J, Czerwiec F, Kambayashi J, Zampino M, et al. Vasopressin V2-receptor blockade with tolvaptan in patients with chronic heart failure: results from a double-blind, randomized trial. Circulation. 2003;107(21):2690–6.
12. Gheorghiade M, Konstam MA, Burnet JC Jr, Grinfeld L, Maggioni AP, Swedberg K, et al. Short-term clinical effects of tolvaptan, an oral vasopressin antagonist, in patients hospitalized for heart failure: the EVEREST clinical status trials. JAMA. 2007;297(12):1332–43.
13. Konstam MA, Gheorghiade M, Burnett JC Jr, Grinfeld L, Maggioni AP, Swedberg K, et al. Effects of oral tolvaptan in patients hospitalized for worsening heart failure: the EVEREST outcome trial. JAMA. 2007;297(12):1319–31.
14. Schrier RW, Gross P, Gheorghiade M, Berl T, Verbalis JG, Czerwiec FS, et al. Tolvaptan, a selective oral vasopressin V2-receptor antagonist, for hyponatremia. N Engl J Med. 2006;355:2099–112.
15. Lin SH, Hsu YJ, Chiu JS, Chu SJ, Davids MR, Halperin ML, et al. Osmotic demyelination syndrome: a potentially avoidable disaster. Q J Med. 2003;96:935–47.
16. Verbalis JG, Goldsmith SR, Greenberg A, Schrier RW, Sterns RH, et al. Hyponatremia treatment guidelines 2007: expert panel recommendations. Am J Med. 2007;120(11 Suppl 1):S1–21.

Disease Models & Mechanisms 3, 431-440 (2010) doi:10.1242/dmm.002311

RESEARCH ARTICLE

Medaka as a model for human nonalcoholic steatohepatitis

Toshihiko Matsumoto[1], Shuji Terai[1,*], Toshiyuki Oishi[1], Shinya Kuwashiro[1], Koichi Fujisawa[1], Naoki Yamamoto[1], Yusuke Fujita[2], Yoshihiko Hamamoto[2], Makoto Furutani-Seiki[3], Hiroshi Nishina[4] and Isao Sakaida[1]

SUMMARY

The global incidence of nonalcoholic steatohepatitis (NASH) is increasing and current mammalian models of NASH are imperfect. We have developed a NASH model in the ricefish medaka (*Oryzias latipes*), which is based on feeding the fish a high-fat diet (HFD). Medaka that are fed a HFD (HFD-medaka) exhibited hyperlipidemia and hyperglycemia, and histological examination of the liver revealed ballooning degeneration. The expression of lipogenic genes (*SREBP-1c*, *FAS* and *ACC1*) was increased, whereas the expression of lipolytic genes (*PPARA* and *CPT1*) was decreased. With respect to liver fatty acid composition, the concentrations of n-3 polyunsaturated fatty acids (PUFAs) and n-6 PUFAs had declined and the n-3:n-6 ratio was reduced. Treatment of HFD-medaka with the n-3 PUFA eicosapentaenoic acid (EPA) mitigated disease, as judged by the restoration of normal liver fatty acid composition and normal expression levels of lipogenic and lipolytic genes. Moreover, medaka that were fed a diet deficient in n-3 PUFAs developed NASH features. Thus, NASH can be induced in medaka by a HFD, and the proportion of n-3 PUFAs in the liver influences the progress of NASH pathology in these fish. Our model should prove helpful for the dissection of the causes of human NASH and for the design of new and effective therapies.

INTRODUCTION

Nonalcoholic fatty liver disease (NAFLD) is the general term for fatty liver diseases that are not the result of a history of alcohol consumption. NAFLD is the most common cause of human liver dysfunction, and it is estimated that about 30% of the general population in the USA suffers from excessive fat accumulation in the liver (Browning et al., 2004). The incidence of NAFLD, which has been increasing in recent years, is closely tied to obesity, diabetes, hyperlipidemia and insulin resistance. Indeed, NAFLD is considered to be a manifestation of metabolic syndrome in the liver (Powell et al., 1990; Sanyal, 2002). NAFLD can be broadly divided into two subgroups: (1) non-progressive simple steatosis, and (2) nonalcoholic steatohepatitis (NASH) with ballooning degeneration and fibrosis (Schaffner and Thaler, 1986; Younossi et al., 1998; Brunt et al., 1999; Matteoni et al., 1999). In cases of progressive chronic liver disease, NASH may progress from steatohepatitis to liver cirrhosis, and may eventually lead to hepatocellular carcinoma.

There have been many attempts to create NASH models in rodents through the use of either genetic mutation, or dietary or pharmacological manipulation (Anstee and Goldin, 2006). The medaka (*Oryzias latipes*) is a small freshwater fish found in Japan and Asia. This member of the ricefish family has a history of use as an animal model in Japan and a number of purebred strains exist (Masahito et al., 1989). Medaka compare favorably to rodents as experimental animals for drug screening because medaka have a high reproductive rate, mature rapidly, and cost little in terms of rearing space and daily maintenance owing to their small size. Sequencing of the medaka genome has been completed and techniques for producing transgenic and knockout animals have been established (Kasahara et al., 2007; Yamauchi et al., 2000). Physiologically, medaka are omnivores and metabolize sugars and lipids in a manner analogous to that of mammals (Sheridan, 1988; Brown and Tappel, 1959). However, despite their metabolic similarities to humans, medaka have not been used previously for NASH research. In this study, we fed a HFD to medaka to induce NASH and determined whether the progression of liver disease in these fish was similar to the progression of human NASH. In addition, we used our medaka NASH model to verify the efficacy of the administration of the n-3 polyunsaturated fatty acid (PUFA) eicosapentaenoic acid (EPA) as a NASH therapy. Our results have shed much-needed light on the mechanisms potentially underlying NASH in humans, and may point to new avenues of therapy for this debilitating disorder.

RESULTS

Gross anatomical and histopathological evidence for NASH in medaka

For an animal model to be useful for determining the molecular and cellular basis of NASH, it must show the same metabolic abnormalities as the human disease. These anomalies include obesity and insulin resistance; liver damage owing to 'fatty liver' and hyperlipidemia; macrovesicular fat deposition in the liver; infiltration by inflammatory cells; and ballooning degeneration of hepatocytes. Like mammals, medaka have livers, gall bladders, digestive tracts and other internal organs in the peritoneum (Fig. 1A,B). In normal medaka liver tissue, the hepatocytes are arranged

[1]Department of Gastroenterology and Hepatology, Yamaguchi University Graduate School of Medicine, Minami Kogushi 1-1-1, Ube, Yamaguchi 755-8505, Japan
[2]Department of Computer Science and Systems Engineering, Faculty of Engineering, Yamaguchi University, Tokiwadai 2-16-1, Ube, Yamaguchi 755-8505, Japan
[3]Centre for Regenerative Medicine, Department of Biology and Biochemistry, University of Bath, Claverton Down, Bath BA2 7AY, UK
[4]Department of Developmental and Regenerative Biology, Medical Research Institute, Tokyo Medical and Dental University, 1-5-45, Yushima, Bunkyo-ku, Tokyo 113-8510, Japan
*Author for correspondence (terais@yamaguchi-u.ac.jp)

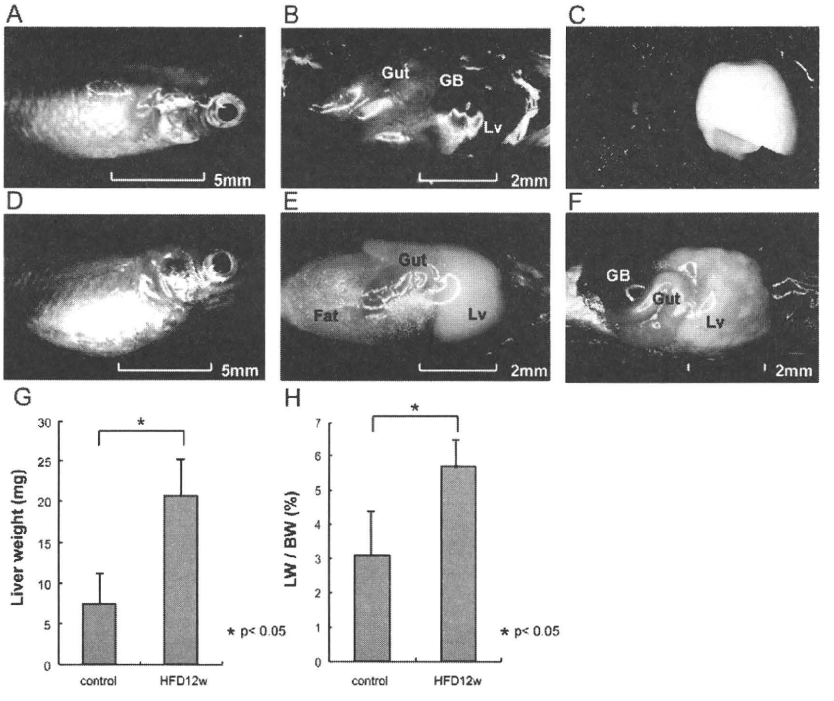

Fig. 1. Altered gross phenotype and liver parameters in HFD-medaka. (A,B) Gross appearance of the abdomen (A) and internal organs (B) of medaka that were fed a control diet for 12 weeks. The abdomen is flat, the liver is brown, and very little visceral fat is observed. Lv, liver; GB, gall bladder; Gut, digestive tract. (C) A comparison of liver color and size in control medaka (left) and HFD-medaka (right). (D,E) Gross appearance of the abdomen (D) and internal organs (E) of medaka that were fed a HFD for 12 weeks. Distention of the abdomen, swelling and whitening of the liver, and a clear increase in visceral fat are seen. (F) Edematous degeneration of the liver in HFD-medaka after 12 weeks. (G,H) Medaka were fed the control diet or the HFD (HFD12w) for 12 weeks, and absolute liver weights (G) and liver weight as a percentage of total body weight (LW/BW) (H), were determined (n=10/group). The results shown in all figure panels are representative of at least three independent trials.

in sheets that are separated by a sinusoidal mesh. Histological examination of normal medaka liver shows that the portal vein, hepatic artery and bile duct are independent, as they are not organized in portal triads (Fig. 2A).

To induce NASH in medaka, 8-week-old fish (n=14/group) were fed either a control diet or a high-fat diet (HFD) for 12 weeks, and monitored for gross anatomical and histological changes at 4, 8 and 12 weeks after HFD initiation. Control medaka grew normally over the 12-week period, from 95±17 mg to 241±32 mg. By contrast, all 14 fish that were fed the HFD exhibited significantly greater body weights, reaching 368±80 mg by the end of the 12 weeks (P<0.05). HFD-medaka also showed distention of the abdomen, owing to increased fat deposition in the viscera, and the presence of a white, swollen liver (Fig. 1C-E). Edematous degeneration of the liver was observed in five out of 14 (36%) HFD-medaka (Fig. 1F). The mean liver weight (Fig. 1G) and the mean liver weight:body weight ratio (Fig. 1H) of HFD-medaka were increased by 2.8-fold and 1.8-fold, respectively, compared with controls, consistent with the observed hepatomegaly in HFD-medaka. Lastly, the weight of intrahepatic total lipids in the HFD-medaka was 6.2-fold greater than in controls (Table 1).

Compared with medaka that were fed a control diet, medaka fed the HFD for 4 weeks exhibited considerably more macrovesicular fat deposition around the hepatic veins (data not shown). By 8 weeks, fat deposition had spread over the entire liver (Fig. 2B; compare with Fig. 2A). By 12 weeks, focal ballooning degeneration and inflammatory cell infiltration in the livers of HFD-medaka were prominent (Fig. 2C,D), consistent with the edematous liver degeneration noted upon gross examination (Fig. 1F). Histopathologically, nine out of 14 (64%) and four out of 14 (29%) HFD-medaka displayed steatohepatitis and simple steatosis, respectively. Liver fibrosis (Fig. 2E,F) and fat accumulation (Fig. 2G) were also observed in these fish. Electron microscopic examination of liver cells from HFD-medaka revealed the presence of lipid droplets (Fig. 2H,I), and the ballooning hepatocytes showed cytoplasmic vacuolation and enlarged lysosomes (Fig. 2H,J).

HFD-medaka show hyperglycemia, hyperlipidemia and altered expression of lipogenic genes

A two-hit theory has been proposed as the mechanism underlying the onset of NASH (Day and James, 1998). The first hit involves increased expression of fatty acid transport-related and lipogenic genes that alter the lipid metabolism inside the liver, such that the liver becomes steatotic. The second hit takes the form of inflammatory cytokines and oxidative stress that drive inflammation and fibrosis. To determine whether a classical first hit was occurring in our HFD-medaka, we analyzed serum components of these fish. Triglyceride (TG) levels in HFD-medaka serum were significantly elevated over those in controls by 4 weeks, and were sevenfold greater by 12 weeks (Fig. 3A). When we analyzed these serum TGs by high-performance liquid chromatography (HPLC), we found that very low-density lipoprotein triglyceride (VLDL-TG) was increased by 15-fold in the serum from HFD-medaka at 12 weeks (2362 mg/dl) compared with controls (160 mg/dl) (Fig. 3B). These results suggested that the HFD-medaka were experiencing an increase in endogenous fatty acid synthesis by hepatocytes. As shown in Fig. 3C, plasma glucose levels were also significantly elevated in HFD-medaka at 8 weeks, and were fourfold greater than in controls by 12 weeks. Serum alanine aminotransferase (ALT) levels were elevated the most (3.7-fold) in HFD-medaka at 4 weeks, but continued to be significantly increased compared with controls at 12 weeks (Fig. 3D). These altered serum parameters parallel our histological examinations of HFD-medaka, in which steatosis was seen at 4 weeks, macrovesicular fat deposition was widespread at 8 weeks, and ballooning degeneration was observed at 12 weeks. Taken together,

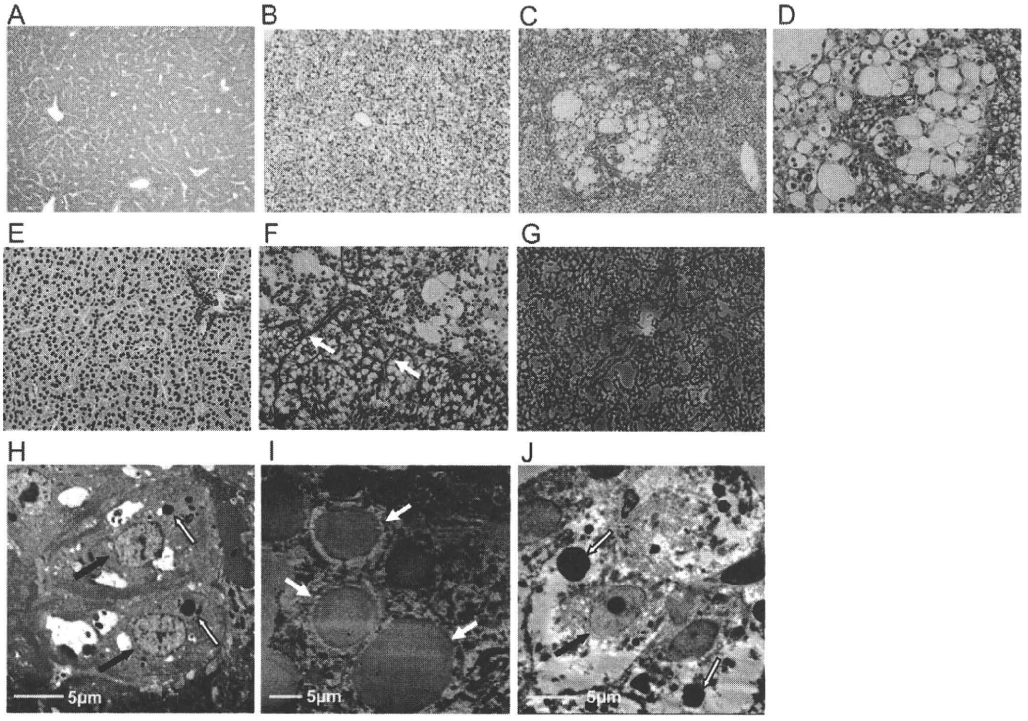

Fig. 2. Altered histopathology in medaka with HFD-induced steatohepatitis. (A) Hematoxylin and eosin (H&E)-stained section of a normal liver from a medaka that was fed the control diet for 12 weeks. The hepatocytes are arranged in sheets separated by a sinusoidal mesh. The portal vein, hepatic artery and bile duct are independent. Magnification ×200. (B) H&E-stained section of a liver from a medaka fed the HFD for 8 weeks. Macrovesicular fat deposition can be seen throughout the entire liver. Magnification ×200. (C,D) H&E-stained section of a liver from HFD-medaka after 12 weeks. In addition to macrovesicular fat deposition, focal ballooning degeneration of hepatocytes accompanied by the infiltration of inflammatory cells can be seen. Magnification ×200 (C); ×400 (D). (E) Gitter staining of the liver from a control medaka at 12 weeks. Magnification ×400. (F) Gitter staining of the liver from a HFD-medaka at 12 weeks. The arrows indicate sinusoidal fibrosis. Magnification ×400. (G) Oil Red O staining of intracellular lipids in the liver of a HFD-medaka at 12 weeks. Magnification ×400. (H) Electron microscopic image of the control medaka in A. Black arrows indicate the nucleus; white arrows indicate the lysosomes. (I) Electron microscopic image of the HFD-fed medaka in B. Arrows indicate hepatocytes loaded with lipid droplets. (J) Electron microscopic image of ballooning degeneration of hepatocytes in the HFD-fed medaka in C. Cytoplasmic vacuolation and enlarged lysosomes can be seen. The black arrow indicates a nucleus; white arrows indicate lysosomes. For A-F, the results shown are representative of 14 medaka examined/group.

these data suggest that a first hit of hyperlipidemia, hyperglycemia and hepatic steatosis occurred in HFD-medaka, followed by a second hit of liver dysfunction owing to ballooning hepatocyte degeneration. Thus, our observations are consistent with the two-hit theory of human NASH development, in which a metabolic abnormality sets the stage for the development of NASH symptoms.

To investigate, at a molecular level, the changes in the fatty acid metabolism of medaka liver during fatty acid loading periods, we used reverse transcription (RT)-PCR to analyze the mRNA expression levels of genes associated with fatty acid synthesis and oxidation. These genes included the main regulator of fatty acid synthesis, sterol regulatory element-binding protein-1c (*SREBP-1c*); the target genes of SREBP-1c, fatty acid synthase (*FAS*) and acetyl-CoA carboxylase 1 (*ACC1*); the main regulator of fatty acid β-oxidation, peroxisome proliferator-activated receptor α (*PPARA*); the mitochondrial β-oxidation marker carnitine palmitoyltransferase 1 (*CPT1*); and the peroxisome β-oxidation marker acyl-CoA oxidase 1 (*ACO1*). Compared with controls, the mRNA expression levels of *SREBP-1c*, *FAS* and *ACC1* were all elevated in HFD-medaka liver at 4 weeks (Fig. 3E, left), confirming that fatty acid synthesis had accelerated in these animals. Conversely, we observed decreased expression of *PPARA* and *CPT1*, but increased expression of *ACO1* (Fig. 3E, right), indicating decreased mitochondrial β-oxidation and accelerated peroxisomal β-oxidation in the HFD-medaka liver. Taken together, these data suggest that HFD-medaka suffer from increased fatty acid synthesis accompanied by decreased fatty acid β-oxidation and inflammation, accounting for their swollen, fatty livers.

To investigate the abnormal fatty acid deposition observed in the HFD-medaka liver, we compared the composition of the fats in control livers with HFD-medaka livers (Table 1). Oleic acid (C18:1n-9) levels in HFD-medaka were clearly higher than in controls, whereas linoleic acid (C18:2n-6), arachidonic acid (C20:4n-6), α-linolenic acid (C18:3n-3), EPA (C20:5n-3) and docosahexaenoic acid (DHA) (C22:6n-3) levels were lower. Although concentrations of both n-3 PUFAs and n-6 PUFAs had declined, the n-3:n-6 ratio was reduced in HFD-medaka because the decrease in n-3 PUFAs was greater than the decrease in n-6 PUFAs. These results are consistent with features of human NASH, in which PUFA levels and n-3:n-6 PUFA ratios are reportedly low in the liver (Araya et al., 2004; Puri et al., 2007). Interestingly, levels of mead acid (C20:3n-9), a marker of essential fatty acid deficiency, were increased in HFD-medaka liver.

Table 1. Fatty acid composition of total lipids in the livers of control, HFD-medaka and HFD+EPA medaka

Fatty acid	Control (molecule %)	HFD (molecule %)	HFD+EPA (molecule %)
C14:0	3.0±0.7	2.1±0.5*	1.4±0.1†
C16:0	26.7±2.1	15.5±2.5*	18.6±2.9†
C18:0	8.7±0.3	2.7±0.9*	3.7±0.6$^{\dagger\#}$
C16:1n-7	4.6±0.4	9.6±0.6*	6.4±0.1$^{\dagger\#}$
C18:1n-9	16.0±1.7	62.5±4.0*	50.4±2.6$^{\dagger\#}$
C20:3n-9	0.2±0.1	1.2±0.3*	0.1±0.1$^{\#}$
C18:2n-6	4.9±0.8	3.9±0.5*	8.4±1.1$^{\dagger\#}$
C18:3n-6	0.5±0.2	1.1±0.4*	1.8±0.1$^{\dagger\#}$
C20:3n-6	0.6±0.4	0.3±0.1	0.1±0.1$^{\dagger\#}$
C20:4n-6	3.0±0.2	1.3±0.4*	0.2±0.1$^{\dagger\#}$
C18:3n-3	0.7±0.2	0.1±0.1*	0.2±0.1$^{\dagger\#}$
C20:5n-3	1.8±0.2	0.1±0.1*	2.1±0.5$^{\#}$
C22:6n-3	23.7±0.7	0.7±0.3*	4.3±1.0$^{\dagger\#}$
Total SFA	38.9±1.6	21.0±3.2*	23.9±3.6†
Total MUFA	22.0±2.1	70.2±3.0*	57.3±2.7$^{\dagger\#}$
Total PUFA	38.9±0.6	7.6±0.2*	18.7±1.1$^{\dagger\#}$
n-3 PUFA	29.5±0.2	0.7±0.3*	8.0±2.0$^{\dagger\#}$
n-6 PUFA	9.4±0.3	6.9±0.3*	10.7±1.0$^{\#}$
n-3:n-6 ratio	3.1±0.1	0.2±0.1*	1.0±0.1$^{\dagger\#}$
Total lipid (mg/g of tissue)	27±9	167±62*	87±28$^{\dagger\#}$

All values are means (molecule %) ± S.E.M. SFA, saturated fatty acid; MUFA, monounsaturated fatty acid; PUFA, polyunsaturated fatty acid. n=6/group; *P<0.05 versus control, $^{\dagger}P$<0.05 versus control, $^{\#}P$<0.05 versus HFD.

EPA treatment inhibits NASH development in medaka

Because administration of the n-3 PUFA EPA has been investigated as a therapy for human NASH, we explored whether EPA treatment could slow disease progression in our medaka NASH model. Medaka were fed a HFD with or without EPA for 12 weeks. The HFD+EPA medaka showed increased fat deposition in the internal organs and a white, swollen liver similar to that observed in the HFD group (Fig. 4A). However, histological examination revealed that the degree of fat deposition in the HFD+EPA group appeared to be less than that in the HFD group during the same period (Fig. 4B). Indeed, analysis of total lipids showed that the fat levels in the HFD+EPA liver were 48% lower than in the HFD liver (Table 1). Moreover, unlike HFD-medaka, the HFD+EPA medaka were not hyperglycemic after fasting (Fig. 4C). HLPC analysis showed that serum TG and VLDL-TG levels were 16% (3132 vs 2643 mg/dl) and 21% (2362 vs 1873 mg/dl) lower in HFD+EPA livers compared with HFD livers, respectively (Fig. 4D). EPA treatment increased EPA (C20:5n-3) and DHA (C22:6n-3) levels, as well as the n-3:n-6 PUFA ratio, in the liver (Table 1). Finally, mead acid (C20:3n-9) levels were decreased in HFD+EPA livers compared with HFD livers (Table 1), suggesting that any essential fatty acid deficiencies that were present had been mitigated.

With respect to gene expression, the levels of *SREBP-1c*, *FAS* and *ACC1* mRNAs were reduced in HFD+EPA medaka compared with HFD-medaka, and the accelerated fatty acid synthesis caused by HFD consumption was abrogated (Fig. 4E, top). By contrast, the levels of *PPARA* and *CPT1* expression were increased, *ACO1* expression was decreased, and markers of mitochondrial β-oxidation became predominant in the HFD+EPA liver (Fig. 4E, bottom). Thus, the pattern of gene expression in livers of HFD+EPA medaka was essentially the same as that in medaka fed the control diet. These data indicate that de novo fatty acid synthesis in HFD-medaka liver decreases upon EPA treatment, and that normal fat utilization is restored.

n-3 PUFA deficiency induces NASH

It has been reported that liver PUFA levels and n-3:n-6 PUFA ratios are low in NASH patients (Araya et al., 2004; Puri et al., 2007). We therefore investigated whether a deficiency in n-3 PUFA could induce NASH in medaka. We prepared an n-3 PUFA-deficient (n-3PUFA^{-}) diet with about the same energy content as the control diet, and used it to feed medaka for 8 weeks. Compared with controls, the n-3PUFA^{-} medaka showed moderate increases in fat deposition in internal organs, and their livers, although pink, were swollen (Fig. 5A). By gross observation, five out of ten (50%) n-3PUFA^{-} medaka showed edematous degeneration of the liver, and histopathological examination revealed that steatohepatitis was present in seven out of ten (70%) of these animals (Fig. 5B). The mean serum ALT value in n-3PUFA^{-} medaka was 442±228 IU/l (Fig. 5C), confirming the presence of liver damage. Thus, NASH is induced in medaka by conditions of n-3PUFA deficiency.

DISCUSSION

Medaka compare favorably to rodents as experimental animals for drug screening because medaka have a high reproductive rate, mature rapidly, and cost little in terms of rearing space and daily maintenance owing to their small size. Our results show that NASH can be induced in medaka by feeding a HFD, and that the development of NASH can be largely prevented by EPA administration. Importantly, we have also demonstrated that n-3 PUFA deficiency can induce NASH in medaka.

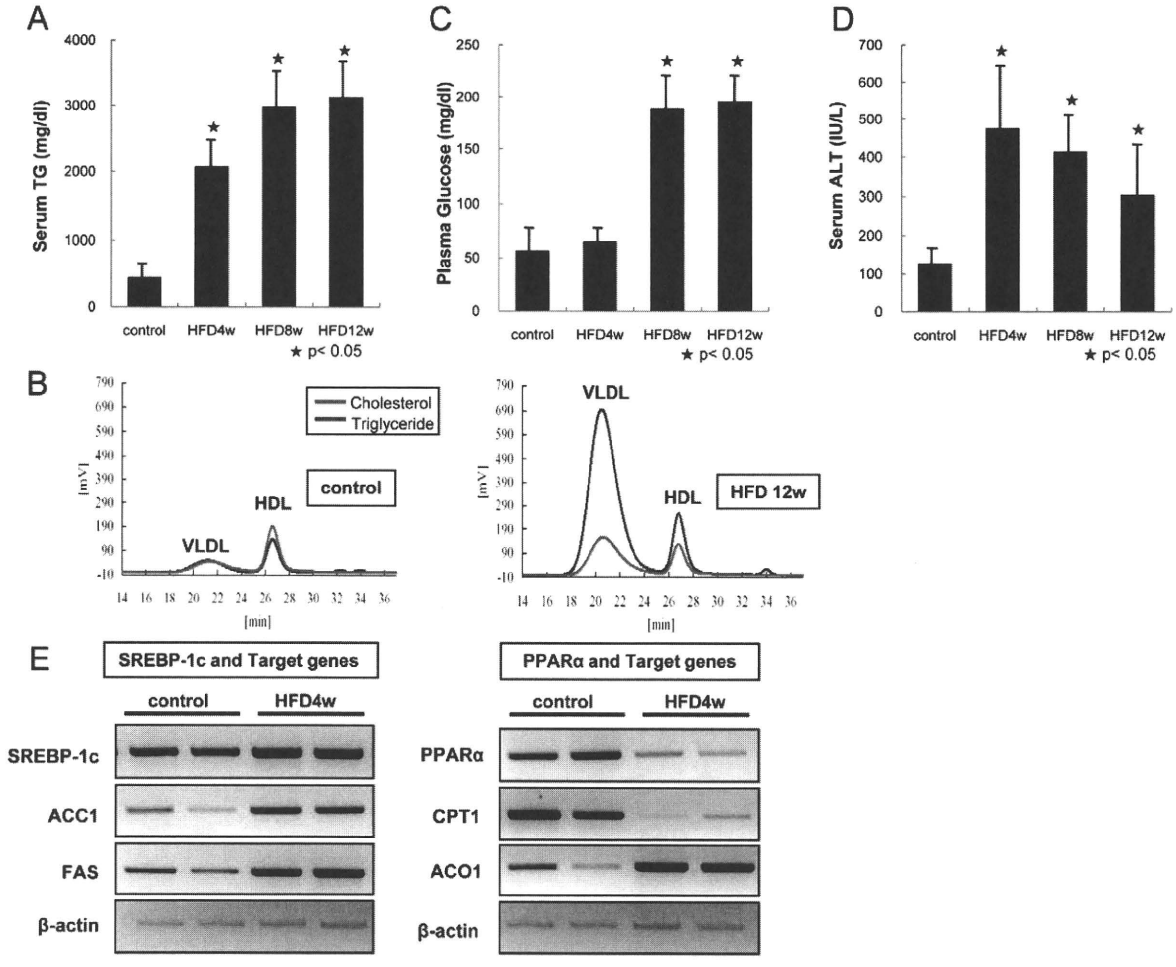

Fig. 3. HFD induces hyperglycemia, hyperlipidemia and the expression of lipogenic genes. (A) Increased TGs. After 12 hours of fasting, serum TG levels were measured in control and HFD-medaka at 4, 8 and 12 weeks. A significant elevation in serum TGs in HFD-medaka was seen by as early as 4 weeks on a HFD (n=10/group). (B) Increased VLDL and high-density lipoprotein (HDL). Serum samples from control (left) and HFD-medaka (right) at 12 weeks were fractionated by HPLC to detect cholesterol and TG levels (n=10/group). A 15-fold increase in serum VLDL-TG was observed in HFD-medaka compared with controls. (C) Increased fasting blood sugar. Plasma glucose was measured in the medaka in A after 12 hours of fasting. Plasma glucose was fourfold higher in the HFD-medaka liver than in controls at 12 weeks (n=12/group). (D) Increased ALT. Serum ALT was measured in the medaka in A and was found to be elevated most highly after 4 weeks on a HFD (n=10/group). (E) Altered expression of lipogenic (left) and lipolytic (right) genes. mRNA levels of the indicated genes in livers from control and HFD-medaka at 4 weeks were determined by semi-quantitative RT-PCR. *SREBP-1c*, *ACC1* and *FAS* were all elevated in HFD-medaka compared with control medaka. Conversely, the mRNA levels of *PPARA* and *CPT1* were reduced and *ACO1* was increased (n=6/group).

We were able to induce steatohepatitis in medaka through feeding, thus creating a NASH model that is easily established in a relatively short period of time. The features of our model include the efficient induction of ballooning degeneration, a key feature in the diagnosis of human NASH (Brunt et al., 1999; Matteoni et al., 1999; Neuschwander-Tetri and Caldwell, 2003). The frequency of ballooning degeneration in normal medaka is 10-20% (Bunton, 1990; Boorman et al., 1997; Brown-Peterson et al., 1999), whereas our HFD-medaka showed a ballooning degeneration frequency of greater than 60%. By contrast, Deng et al. have shown that 46% of C57BL/6 mice fed a HFD through an implanted gastrostomy tube develop steatohepatitis (Deng et al., 2005). Thus, our medaka model of NASH induction is slightly superior to the mouse model in terms of the efficiency of ballooning degeneration induction (64% vs 46%).

The mechanisms underlying the digestion and absorption of lipids; the transport of exogenous and endogenous lipids; and fatty acid oxidation are almost identical in fish and mammals (Brown and Tappel, 1959; Sheridan, 1988). However, there are some differences in how fatty acids are released from intestinal epithelial cells into blood vessels or lymph ducts (Sheridan, 1988). In mammals, short chain fatty acids (SCFAs) and medium chain fatty acids (MCFAs) that are absorbed by intestinal epithelial cells are released directly into the portal vein without esterification. Most long chain fatty acids (LCFAs) are resynthesized into TGs and released into lymph ducts as chylomicron particles, but some are released into the portal vein without esterification. In fish, LCFAs are rapidly processed into free fatty acids (FFAs), and only later are resynthesized as TGs and released as chylomicron

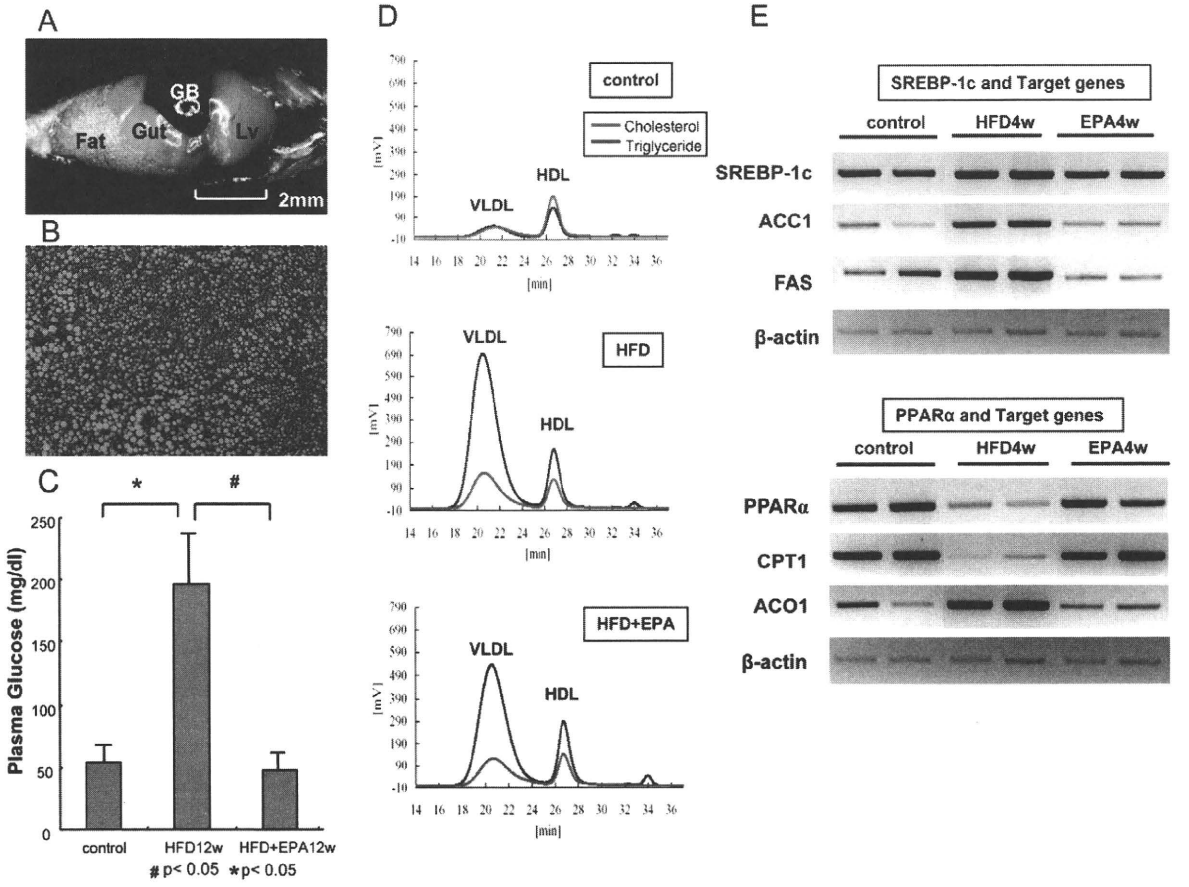

Fig. 4. EPA treatment inhibits NASH development in medaka. (A) Gross appearance of the abdomen from an HFD+EPA medaka. A white, swollen liver and increased visceral fat are visible in the HFD+EPA medaka after 12 weeks on a HFD. (B) Ameliorated histopathology. An H&E-stained section of a liver from an HFD+EPA medaka at 12 weeks. Macrovesicular fat deposition can be seen but there is very little ballooning degeneration. (C) Normal fasting blood sugar. After 12 hours of fasting, the plasma glucose level of HFD+EPA medaka at 12 weeks was the same as that in controls. The hyperglycemia that was evident in HFD-medaka at 12 weeks was not observed. (D) Decreased TG. Serum samples from control, HFD-medaka and HFD+EPA medaka at 12 weeks were analyzed by HPLC as for Fig. 3B. HFD+EPA medaka showed a 21% decrease in serum VLDL-TG compared with HFD-medaka. For A-D, the results shown are representative of 10-12 individuals that were examined/group. (E) Restored gene expression. mRNA levels of the indicated lipogenic and lipolytic genes were examined in control, HFD-medaka and HFD+EPA medaka at 4 weeks by semi-quantitative RT-PCR as for Fig. 3E. Compared with HFD-medaka, the mRNA levels of *SREBP-1c*, *ACC1* and *FAS* were reduced in HFD+EPA medaka and resembled those in medaka that were fed the control diet. Conversely, the expression levels of *PPARA* and *CPT1* were increased in HFD+EPA medaka, whereas the level of *ACO1* was decreased. This pattern also resembled that observed in medaka that were fed the control diet (*n*=6/group).

particles into the blood (Robinson and Mead, 1973; Sheridan, 1988). Our medaka NASH model was created by feeding a HFD based on LCFAs, and we believe that many of the consumed LCFAs arrive in the liver as FFA-albumin complexes. In obese humans that develop NASH, insulin signaling in adipocytes is disrupted such that hormone-sensitive lipases hydrolyze TGs into fatty acids (Hotamisligil et al., 1995). These fatty acids are subsequently released from the adipocytes and enter the liver through the portal vein, exacerbating NASH development (Hotamisligil et al., 1995; Day, 2002). We believe that a similar scenario occurs in our HFD-medaka, such that FFAs derived from consumed LCFAs flow into the liver. After obesity develops in medaka, FFAs from fat tissues may also join this flow, perhaps explaining why NASH develops more easily in medaka than in other animal models.

In contrast to the lipids of terrestrial vertebrates, fish lipids contain a high proportion of PUFAs, particularly the n-3 PUFAs whose function is to maintain lipid liquidity at low temperature. However, as with terrestrial mammals, fish are unable to synthesize n-6 and n-3 PUFAs, making these molecules essential fatty acids that must be consumed. The HFD used in our study included 64.9% oleic acid, 12.8% palmitic acid (C16:0), 7.6% stearic acid (C18:0), 10.3% linoleic acid and 0.2% α-linolenic acid. Monounsaturated fatty acids (MUFAs) and saturated fatty acids (SFAs) accounted for most of the fatty acids, with only an extremely small proportion of α-linolenic acid being present. The synthesis of highly unsaturated fatty acids (HUFAs), such as arachidonic acid, EPA, DHA and other fatty acids with a carbon chain length of greater than 20, depends on the action of delta-6 and delta-5 desaturases (Sprecher, 1981). These enzymes preferentially desaturate n-3PUFAs then n-6PUFAs

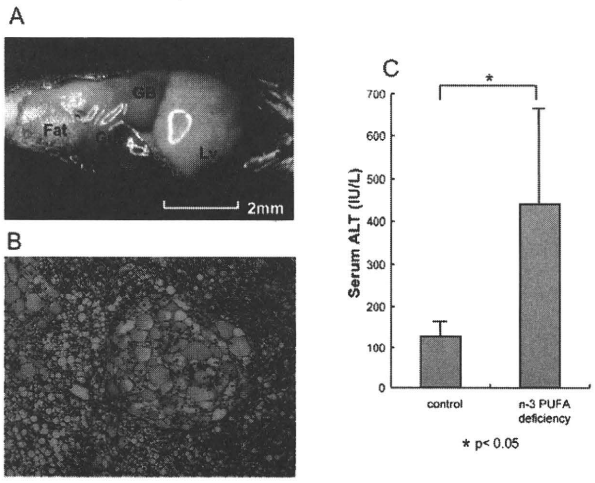

Fig. 5. n-3 PUFA deficiency induces NASH in medaka. (A) Gross appearance of the abdomen. Edematous degeneration accompanying liver swelling and a slight increase in visceral fat is observed in medaka fed an n-3 PUFA-deficient (n-3PUFA$^-$) diet for 8 weeks. (B) An H&E-stained section of liver from an n-3 PUFA$^-$ medaka. Macrovesicular fat deposition is visible throughout the liver, as is focal ballooning degeneration. For A and B, the results shown are representative of ten individuals that were examined/group. (C) Serum ALT values of the n-3 PUFA$^-$ medaka in A and B were twofold to fourfold higher than those in medaka that were fed the control diet (n=10/group).

Table 2. Composition of control, HFD and n-3 PUFA-deficient diets

Diet	Grams/100 g	Calorie %	Kcal/100 g
Control diet			
Protein	50.0	62.5	200.0
Fat	9.0	25.3	81.0
Carbohydrates	11.0	13.8	44.0
Total			325.0
n-3 PUFA-deficient diet			
Protein	21.5	23.9	86.0
Fat	4.4	11.0	39.6
Carbohydrates	58.6	65.1	234.4
Total			360.0
HFD diet			
Protein	25.5	20.1	102.0
Fat	32.0	56.7	288.0
Carbohydrates	29.4	23.2	117.6
Total			507.6

and then n-9PUFAs in a process that is controlled by HUFAs (Cho et al., 1999). Thus, EPA and DHA levels and n-3:n-6 PUFA ratios declined in our HFD-medaka owing to their greatly reduced consumption of α-linolenic acid, EPA and DHA. By contrast, the levels of mead acid increased in HFD-medaka owing to the desaturation of oleic acid. In HFD-medaka treated with EPA, the increased levels of EPA and DHA in the liver probably inhibited the activity of delta-6 and delta-5 desaturases. As a result, the conversion of linoleic acid to arachidonic acid, as well as that of oleic acid to mead acid, was inhibited.

The n-3 PUFAs are ligands for PPARα, and PPARα activation increases the expression of fatty acid oxidation enzymes such that fatty acid oxidation is promoted (Gottlicher et al., 1992; Forman et al., 1997; Ren et al., 1997). Therefore, when PUFAs are deficient, fatty acid oxidation declines and livers accumulate fat (Fukazawa et al., 1971). In our medaka NASH model, expression of the mRNA encoding the lipogenic transcription factor SREBP-1c was induced, and expression levels of the fatty acid synthesis pathway enzymes ACC1 and FAS were increased. Conversely, expression levels of the lipolytic transcription factor PPARα, as well as those of CPT1 (the rate-limiting enzyme in mitochondrial β-oxidation), were reduced. Concomitantly, the expression of ACO1, which is involved in peroxisome β-oxidation, was increased. The observed reduction in CPT1 expression may be attributable to the production of malonyl CoA, an intermediate product of fatty acid synthesis. Malonyl CoA interferes with CPT1 expression, and it is thought that compensatory peroxisome β-oxidation is induced (McGarry et al., 1977).

In humans, n-3 PUFA deficiency has been linked to neuropathy and immune system impairment (Holman, 1998). Variations in n-3 PUFA concentrations in the liver may thus indirectly regulate the inflammation associated with NASH. The notion that n-3 PUFAs are involved in the pathology seen in our medaka NASH model is supported by the observation that the expression levels of genes involved in fatty acid metabolism were restored to control levels when HFD-medaka were treated with EPA.

In conclusion, our study shows that the induction of fatty liver and the reproduction of NASH pathology in medaka can be achieved by feeding a diet that is low in EPA and DHA, but that has about the same energy content as a control diet. Moreover, our model is easily, cheaply and rapidly established in the laboratory, allowing ample latitude for exploration of its usefulness. We anticipate that our medaka NASH model will indeed be helpful for clarifying human NASH pathology and for assisting in the development of novel therapeutics aimed at preventing or alleviating this burgeoning health problem.

METHODS

Animals

Himedaka strain Cab (an orange-red variety of medaka, *Oryzias latipes*) fish that were 8 weeks old were used for most experiments. Fish were maintained at a stocking level of ten fish/tank in tap water with aeration. The ten fish in a given tank received a daily ration of 200 mg of the diet prescribed for that group, an amount that was consumed completely within 14 hours. All fish were maintained in accordance with the Animal Care Guidelines of Yamaguchi University. During experiments, fish were kept in plastic tanks covered with plastic covers and illuminated with fluorescent light from 8:00 a.m. to 10:00 p.m. The tank water temperature was maintained at 26±1°C.

Diets

The proportions of protein, fat and carbohydrate, as well as the fatty acid compositions, of the control, HFD and n-3 PUFA-deficient diets that were used in this study are shown in Tables 2 and 3. The energy content of the control diet (Hikari Crest; Kyorin Co. Ltd, Hyogo, Japan) was 3.3 kcal/g, with 25.3% of the calories

Table 3. Fatty acid composition of control, HFD and n-3 PUFA-deficient diets

Fatty acid		Control (g/100 g)	HFD (g/100 g)	n-3 PUFA deficiency (g/100 g)
Myristic acid	C14:0	0.42	0.35	0.02
Myristoleic acid	C14:1n-5	0.00	0.10	0.00
Pentadecanic acid	C15:0	0.00	0.03	0.00
Palmitic acid	C16:0	2.11	4.03	0.66
Palmitoleic acid	C16:1n-7	0.50	0.38	0.01
Heptadecanic acid	C17:0	0.00	0.13	0.00
Heptadecenic acid	C17:1	0.00	0.10	0.01
Stearic acid	C18:0	1.03	2.40	0.22
Oleic acid	C18:1n-9	1.38	20.50	0.92
Linoleic acid	C18:2n-6	0.88	3.26	2.31
α-Linolenic acid	C18:3n-3	0.13	0.06	0.22
Arachidic acid	C20:0	0.02	0.10	0.01
Gondoic acid	C20:1n-9	0.19	0.10	0.03
Arachidonic acid	C20:4n-6	0.08	0.00	0.00
Eicosapentaenoic acid	C20:5n-3	0.93	0.00	0.00
Behenic acid	C22:0	0.00	0.06	0.01
Erucic acid	C22:1n-9	0.03	0.00	0.00
Docosapentaenoic acid	C22:5n-3	0.13	0.00	0.00
Lignoceric acid	C24:0	0.02	0.00	0.00
Docosahexaenoic acid	C22:6n-3	1.07	0.00	0.00
Nervonic acid	C24:1n-9	0.04	0.00	0.00
Total (g/100 g)		8.96	31.60	4.42
Total PUFA (g/100 g)		3.22	3.32	2.53
n-3 PUFA (g/100 g)		2.26	0.06	0.22
n-6 PUFA (g/100 g)		0.96	3.26	2.31
n-3:n-6 ratio		2.35	0.02	0.10

from fat, 62.5% of calories from protein, and 13.8% of calories from carbohydrate, plus vitamins and minerals as recommended. The energy content of the high-fat diet (HFD32; CLEA Japan Inc., Tokyo, Japan) was 5.1 kcal/g, with 56.7% of calories from fat, 20.1% of calories from protein, and 23.2% of calories from carbohydrate, plus vitamins and minerals as recommended. The n-3 PUFA-deficient (EPA- and DHA-deficient) diet, which consisted of fish meal-free powder (F1 diet; Funabashi Farm Co. Ltd, Chiba, Japan), had an energy content of 3.6 kcal/g, with 11.0% of calories from fat, 23.9% of calories from protein, and 65.1% of calories from carbohydrate, plus vitamins and minerals as recommended. For EPA treatment, eicosapentaenoic acid ethyl ester (EPA-E, purity >99%; Mochida Pharmaceutical Co. Ltd, Tokyo, Japan) was mixed with HFD32 to a concentration of 5% by weight.

Histology

Euthanized fish were slit open from the anal vent to the gills, and the entire body was fixed with 4% paraformaldehyde in 0.1 M phosphate buffer (Muto, Tokyo, Japan). The liver was dissected, dehydrated in alcohol, and embedded in paraffin according to standard procedures. Serial sections (3-5 μm thick) were cut and stained with hematoxylin and eosin (H&E). Liver fibrosis was assessed by Gitter staining. Intracellular lipids were stained with Oil Red O to analyze fat accumulation in the liver.

Electron microscopy

Chunks of medaka liver were fixed with 2% glutaraldehyde and 4% paraformaldehyde in 0.1 M phosphate buffer for 30 minutes at 4°C. Fixed liver pieces were washed thoroughly in 0.1 M phosphate buffer, post-fixed for 30 minutes with 1% osmium tetraoxide in 0.1 M phosphate buffer, and then block-stained with 2% aqueous uranyl acetate for 30 minutes to enhance the contrast for electron microscopy. Samples were dehydrated through a graded ethanol series, infused with propylene oxide, and embedded in epoxy resin. Ultra-thin sections were collected on copper grids, stained with 2% aqueous uranyl acetate for 8 minutes and 0.5% lead citrate for 8 minutes, followed by examination under a Hitachi H7500 electron microscope.

Blood analysis

Blood samples were obtained from medaka following a 12-hour fast. Fish were kept on ice for 1-2 minutes and then bled by cutting a ventral portion of the tail fin. Blood was collected in a microcapillary tube and the volume measured. Blood samples were kept at room temperature for 1 hour before centrifugation at 1200 × *g* for 30 minutes at 4°C. Serum ALT concentrations were measured using a Fuji Dry-Chem 3500 (Fuji Film Co. Ltd, Tokyo, Japan). Plasma glucose levels were determined using a Glucocard G-meter (Arkray Co. Ltd, Kyoto, Japan). Cholesterol and TG

Table 4. Primers for seven genes examined in the livers of HFD-medaka

Gene	Forward primer (5′ to 3′)	Reverse primer (3′ to 5′)
ACC1	GAGTGACGTCCTGCTTGACA	ACCTTTGGTCCACCTCACAG
ACO1	GCTCAGCTTTACAGCCTTGG	GGACGATTCCCTAACGATCA
CPT1	ATGTCTACCTCCGTGGACGA	CAAGTTTGGCCTCTCCTTTG
FAS	GACGCTTCAGGAAATGGGTA	GGACAGGAACCGGACTATCA
PPARA	TCTTGAGTGTCGGGTGTGTG	CGGTAGAGCCCACCATCTT
SREBP-1c	CCCAACCAGATGAGGAGAAA	AGGACTTTTGTGCTGCTCGT
β-actin	CTGGACTTCGAGCAGGAGAT	GCTGGAAGGTGGACAGAGAG

profiles in total lipoproteins were analyzed using a dual-detection HPLC system (Skylight Biotech, Akita, Japan) with two tandem-connected TSKgel LipopropakXL columns (300 × 7.8 mm; Tosoh, Japan).

Fatty acid analysis

The fatty acid composition of homogenized liver tissue (20 mg tissue/ml saline) was determined by capillary gas chromatography. Total lipids were extracted by Folch's procedure (Folch et al., 1957), and fatty acids were methylated with boron trifluoride and methanol. Methylated fatty acids were analyzed using a Shimadzu GC-17A gas chromatograph (Shimadzu Co. Ltd, Kyoto, Japan) and a BPX70 capillary column (0.25 mm internal diameter × 30 mm; SGE International Ltd, Melbourne, Australia). Tricosanoic acid (C23:0) was used as the internal standard. The minimum detectable fatty acid concentration detected by this assay is 0.5 μg/ml.

Semi-quantitative RT-PCR

To avoid any acute effects of food intake, fish were fasted overnight prior to sacrifice. Livers were isolated and total RNA was extracted and purified using the RNeasy kit (Qiagen, Hilden, Germany). cDNAs were synthesized using purified RNA plus random hexamers and the Transcriptor First Strand cDNA synthesis kit (Roche, Indianapolis, IN). Semi-quantitative RT-PCR was performed using a PCR master mix (Promega, Madison, WI) and the primers listed in Table 4. Gene expression levels were normalized against β-actin (endogenous control).

Statistical analyses

Numerical data are expressed as the mean ± S.D. The Student's *t*-test was performed to assess statistical significance among groups of medaka. *P* values less than 0.05 were considered to be significant.

ACKNOWLEDGEMENTS

This study was supported by Grants-in-Aid for Scientific Research from the Japan Society for the Promotion of Science (Nos. 18590737, 18659209, 19590693, 19390199, 20659116 and 21659189); the Knowledge Cluster Initiative; the Ministry of Health, Labour and Welfare; and Japan Aerospace Exploration Agency (JAXA). We also thank Dr Masaaki Soma and Dr David Tosh for critical reading of the manuscript.

COMPETING INTERESTS

The authors declare no competing financial interests.

AUTHOR CONTRIBUTIONS

T.M., S.T. and I.S. conceived and designed the experiments; T.M., S.K., K.F., T.O. and N.Y. performed the experiments; T.M., Y.F. and Y.H. analyzed the data; M.F.-S. and H.N. contributed reagents, materials and analytical tools; T.M. and S.T. wrote the paper.

Received 25 November 2008; Accepted 29 October 2009.

TRANSLATIONAL IMPACT

Clinical issue

Nonalcoholic fatty liver disease (NAFLD) is the most common cause of human liver dysfunction, and an estimated 30% of the general population of the USA suffer from excessive fat accumulation in the liver. NAFLD is broadly divided into two subgroups: (1) non-progressive simple steatosis, and (2) nonalcoholic steatohepatitis (NASH) with worsening degeneration and fibrosis. In cases of progressive chronic liver disease, NASH may progress from steatohepatitis to liver cirrhosis, and may eventually lead to hepatocellular carcinoma. A lack of knowledge about the mechanisms that lead to NASH progression prevent advances in drug development.

Results

The authors establish a NASH model using the ricefish medaka (*Oryzias latipes*), which were fed a high-fat diet (HFD) for 12 weeks (HFD-medaka). HFD-medaka exhibited hyperlipidemia, hyperglycemia and hepatic steatosis, with progressive hepatocyte degeneration that led to liver dysfunction. These findings are consistent with NASH progression in humans.

Expected genetic changes were also detected in the NASH model, including increased expression of lipogenic genes and decreased expression of lipolytic genes after HFD feeding. The concentrations of n-3 polyunsaturated fatty acids (PUFAs) and n-6 PUFAs declined, and the n-3:n-6 ratio was reduced in HFD-fed animals, which reflects the biochemistry in humans. Treating HFD-fed medaka with a drug used to treat human NASH [n-3 PUFA eicosapentaenoic acid (EPA)] mitigated disease, restoring normal liver fatty acid composition and normal expression levels of lipogenic and lipolytic genes. Moreover, medaka that were fed a diet deficient in n-3 PUFAs developed features of NASH. This NASH model demonstrates that the proportion of n-3 PUFAs that are present in the liver plays an important role in the progress of NASH pathology.

Implications and future directions

The medaka genome was recently sequenced, making it amenable to forward genetic screens with N-ethyl-N-nitrosourea (ENU), and morpholino knockdown. These techniques promote the analysis of specific gene mutations in these fish. Thus, with their high reproductive rate, rapid maturation and low maintenance costs, medaka compare favorably with rodents as experimental animals. This NASH model is a useful tool to study the unknown mechanisms underlying human liver disease, and should eventually be useful for therapeutic screen tests.

doi:10.1242/dmm.005355

REFERENCES

Anstee, Q. M. and Goldin, R. D. (2006). Mouse models in non-alcoholic fatty liver disease and steatohepatitis research. *Int. J. Exp. Pathol.* **87**, 1-16.

Araya, J., Rodrigo, R., Videla, L. A., Thielemann, L., Orellana, M., Pettinelli, P. and Poniachik, J. (2004). Increase in long-chain polyunsaturated fatty acid n-6/n-3 ratio in relation to hepatic steatosis in patients with non-alcoholic fatty liver disease. *Clin. Sci. (Lond.)* **106**, 635-643.

Boorman, G. A., Botts, S., Bunton, T. E., Fournie, J. W., Harshbarger, J. C., Hawkins, W. E., Hinton, D. E., Jokinen, M. P., Okihiro, M. S. and Wolfe, M. J. (1997). Diagnostic criteria for degenerative, inflammatory, proliferative nonneoplastic and neoplastic liver lesions in medaka (Oryzias latipes): consensus of a National Toxicology Program Pathology Working Group. *Toxicol. Pathol.* **25**, 202-210.

Brown, W. D. and Tappel, A. L. (1959). Fatty acid oxidation by carp liver mitochondria. *Arch. Biochem. Biophys.* **85**, 149-158.

Brown-Peterson, N. J., Krol, R. M., Zhu, Y. and Hawkins, W. E. (1999). N-nitrosodiethylamine initiation of carcinogenesis in Japanese medaka (Oryzias latipes): hepatocellular proliferation, toxicity, and neoplastic lesions resulting from short term, low level exposure. *Toxicol. Sci.* **50**, 186-194.

Browning, J. D., Szczepaniak, L. S., Dobbins, R., Nuremberg, P., Horton, J. D., Cohen, J. C., Grundy, S. M. and Hobbs, H. H. (2004). Prevalence of hepatic steatosis in an urban population in the United States: impact of ethnicity. *Hepatology* **40**, 1387-1395.

Brunt, E. M., Janney, C. G., Di Bisceglie, A. M., Neuschwander-Tetri, B. A. and Bacon, B. R. (1999). Nonalcoholic steatohepatitis: a proposal for grading and staging the histological lesions. *Am. J. Gastroenterol.* **94**, 2467-2474.

Bunton, T. E. (1990). Hepatopathology of diethylnitrosamine in the medaka (Oryzias latipes) following short-term exposure. *Toxicol. Pathol.* **18**, 313-323.

Cho, H. P., Nakamura, M. T. and Clarke, S. D. (1999). Cloning, expression, and nutritional regulation of the mammalian Delta-6 desaturase. *J. Biol. Chem.* **274**, 471-477.

Day, C. P. (2002). Pathogenesis of steatohepatitis. *Best Pract. Res. Clin. Gastroenterol.* **16**, 663-678.

Day, C. P. and James, O. F. (1998). Steatohepatitis: a tale of two "hits"? *Gastroenterology* **114**, 842-845.

Deng, Q. G., She, H., Cheng, J. H., French, S. W., Koop, D. R., Xiong, S. and Tsukamoto, H. (2005). Steatohepatitis induced by intragastric overfeeding in mice. *Hepatology* **42**, 905-914.

Folch, J., Lees, M. and Sloane Stanley, G. H. (1957). A simple method for the isolation and purification of total lipides from animal tissues. *J. Biol. Chem.* **226**, 497-509.

Forman, B. M., Chen, J. and Evans, R. M. (1997). Hypolipidemic drugs, polyunsaturated fatty acids, and eicosanoids are ligands for peroxisome proliferator-activated receptors alpha and delta. *Proc. Natl. Acad. Sci. USA* **94**, 4312-4317.

Fukazawa, T., Privett, O. S. and Takahashi, Y. (1971). Effect of EFA deficiency on lipid transport from liver. *Lipids* **6**, 388-393.

Gottlicher, M., Widmark, E., Li, Q. and Gustafsson, J. A. (1992). Fatty acids activate a chimera of the clofibric acid-activated receptor and the glucocorticoid receptor. *Proc. Natl. Acad. Sci. USA* **89**, 4653-4657.

Holman, R. T. (1998). The slow discovery of the importance of omega 3 essential fatty acids in human health. *J. Nutr.* **128**, 427S-433S.

Hotamisligil, G. S., Arner, P., Caro, J. F., Atkinson, R. L. and Spiegelman, B. M. (1995). Increased adipose tissue expression of tumor necrosis factor-alpha in human obesity and insulin resistance. *J. Clin. Invest.* **95**, 2409-2415.

Kasahara, M., Naruse, K., Sasaki, S., Nakatani, Y., Qu, W., Ahsan, B., Yamada, T., Nagayasu, Y., Doi, K., Kasai, Y. et al. (2007). The medaka draft genome and insights into vertebrate genome evolution. *Nature* **447**, 714-719.

Masahito, P., Aoki, K., Egami, N., Ishikawa, T. and Sugano, H. (1989). Life-span studies on spontaneous tumor development in the medaka (Oryzias latipes). *Jpn. J. Cancer Res.* **80**, 1058-1065.

Matteoni, C. A., Younossi, Z. M., Gramlich, T., Boparai, N., Liu, Y. C. and McCullough, A. J. (1999). Nonalcoholic fatty liver disease: a spectrum of clinical and pathological severity. *Gastroenterology* **116**, 1413-1419.

McGarry, J. D., Mannaerts, G. P. and Foster, D. W. (1977). A possible role for malonyl-CoA in the regulation of hepatic fatty acid oxidation and ketogenesis. *J. Clin. Invest.* **60**, 265-270.

Neuschwander-Tetri, B. A. and Caldwell, S. H. (2003). Nonalcoholic steatohepatitis: summary of an AASLD Single Topic Conference. *Hepatology* **37**, 1202-1219.

Powell, E. E., Cooksley, W. G., Hanson, R., Searle, J., Halliday, J. W. and Powell, L. W. (1990). The natural history of nonalcoholic steatohepatitis: a follow-up study of forty-two patients for up to 21 years. *Hepatology* **11**, 74-80.

Puri, P., Baillie, R. A., Wiest, M. M., Mirshahi, F., Choudhury, J., Cheung, O., Sargeant, C., Contos, M. J. and Sanyal, A. J. (2007). A lipidomic analysis of nonalcoholic fatty liver disease. *Hepatology* **46**, 1081-1090.

Ren, B., Thelen, A. P., Peters, J. M., Gonzalez, F. J. and Jump, D. B. (1997). Polyunsaturated fatty acid suppression of hepatic fatty acid synthase and S14 gene expression does not require peroxisome proliferator-activated receptor alpha. *J. Biol. Chem.* **272**, 26827-26832.

Robinson, J. S. and Mead, J. F. (1973). Lipid absorption and deposition in rainbow trout (Salmo gairdnerii). *Can. J. Biochem.* **51**, 1050-1058.

Sanyal, A. J. (2002). AGA technical review on nonalcoholic fatty liver disease. *Gastroenterology* **123**, 1705-1725.

Schaffner, F. and Thaler, H. (1986). Nonalcoholic fatty liver disease. *Prog. Liver Dis.* **8**, 283-298.

Sheridan, M. A. (1988). Lipid dynamics in fish: aspects of absorption, transportation, deposition and mobilization. *Comp. Biochem. Physiol. B* **90**, 679-690.

Sprecher, H. (1981). Biochemistry of essential fatty acids. *Prog. Lipid. Res.* **20**, 13-22.

Yamauchi, M., Kinoshita, M., Sasanuma, M., Tsuji, S., Terada, M., Morimyo, M. and Ishikawa, Y. (2000). Introduction of a foreign gene into medakafish using the particle gun method. *J. Exp. Zool.* **287**, 285-293.

Younossi, Z. M., Gramlich, T., Liu, Y. C., Matteoni, C., Petrelli, M., Goldblum, J., Rybicki, L. and McCullough, A. J. (1998). Nonalcoholic fatty liver disease: assessment of variability in pathologic interpretations. *Mod. Pathol.* **11**, 560-565.

Retinoic Acid Signaling Positively Regulates Liver Specification by Inducing *wnt2bb* Gene Expression in Medaka

Takahiro Negishi,[1,2] Yoko Nagai,[1,2] Yoichi Asaoka,[1] Mami Ohno,[1] Misako Namae,[1] Hiroshi Mitani,[3] Takashi Sasaki,[4] Nobuyoshi Shimizu,[4] Shuji Terai,[5] Isao Sakaida,[5] Hisato Kondoh,[6,7] Toshiaki Katada,[2] Makoto Furutani-Seiki,[6,8]* and Hiroshi Nishina[1]*‡

During vertebrate embryogenesis, the liver develops at a precise location along the endodermal primitive gut tube because of signaling delivered by adjacent mesodermal tissues. Although several signaling molecules have been associated with liver formation, the molecular mechanism that regulates liver specification is still unclear. We previously performed a screen in medaka to isolate mutants with impaired liver development. The medaka *hio* mutants exhibit a profound (but transient) defect in liver specification that resembles the liver formation defect found in zebrafish *prometheus* (*prt*) mutants, whose mutation occurs in the *wnt2bb* gene. In addition to their liver abnormality, *hio* mutants lack pectoral fins and die after hatching. Positional cloning indicated that the *hio* mutation affects the *raldh2* gene encoding retinaldehyde dehydrogenase type2 (RALDH2), the enzyme principally responsible for retinoic acid (RA) biosynthesis. Mutations of *raldh2* in zebrafish preclude the development of pectoral fins. Interestingly, in *hio* mutants, expression of *wnt2bb* in the lateral plate mesoderm (LPM) directly adjacent to the liver-forming endoderm was completely lost. *Conclusion:* Our data reveal the unexpected finding that RA signaling positively regulates the *wnt2bb* gene expression required for liver specification in medaka. These results suggest that a common molecular mechanism may underlie liver and pectoral fin specification during piscine embryogenesis. (HEPATOLOGY 2010;51:1037-1045.)

Embryonic liver development occurs in multiple stages that are governed by hormonal factors as well as by intercellular and matrix–cellular interactions. In mice, liver ontogeny initiates on approximately embryonic day 9 (E9), when epithelial cells of the foregut endoderm interact with the cardiogenic mesoderm and commit to becoming the liver primordium. The liver primordium proliferates and invades the mesenchyme of the septum transversum to give rise to the hepatic codes and bud at E9.5.[1,2] Over the last decade, studies in rats and mice have greatly expanded the list of molecules known to contribute to liver development;

Abbreviations: AP, anteroposterior; atRA, all-trans retinoic acid; ck19, cytokeratin19; cp, ceruloplasmin; E, embryonic day; hio, hiohgi; LPM, lateral plate mesoderm; MO, Morpholino; mRNA, messenger RNA; nls, neckless; nof, no-fin; PED6, N-([6-(2,4-dinitro-phenyl)amino]hexanoyl)-1-palmitoyl-2-BODIPY-FL-pentanoyl-sn-glycero-3-phosphoethanolamine; prt, prometheus; RA, retinoic acid; RALDH2, Retinaldehyde dehydrogenase type2.

From the [1]Department of Developmental and Regenerative Biology, Medical Research Institute, Tokyo Medical and Dental University, Tokyo, Japan; the [2]Department of Physiological Chemistry, Graduate School of Pharmaceutical Sciences, University of Tokyo, Tokyo, Japan; the [3]Department of Integrated Biosciences, Graduate School of Frontier Science, University of Tokyo, Chiba, Japan; the [4]Department of Molecular Biology, Keio University School of Medicine, Tokyo, Japan; the [5]Department of Gastroenterology & Hepatology, Yamaguchi University Graduate School of Medicine, Yamaguchi, Japan; the [6]Japan Science and Technology Agency, Solution Oriented Research for Science and Technology Kondoh Research Team, Kyoto, Japan; the [7]Department of Frontier Biosciences, Graduate School of Frontier Biosciences, Osaka University, Osaka, Japan; and the [8]Centre for Regenerative Medicine, Department of Biology and Biochemistry, University of Bath, Bath, UK.

Received August 11, 2009; accepted October 9, 2009.

Supported by Grants-in-Aid for Scientific Research from the Ministry of Education, Culture, Sport, Science and Technology of Japan and the Ministry of Health, Labor and Welfare of Japan.

Address reprint requests to: Hiroshi Nishina, Department of Developmental and Regenerative Biology, Medical Research Institute, Tokyo Medical and Dental University, 1-5-45, Yushima, Bunkyo-ku, Tokyo 113-8510, Japan. E-mail: nishina.dbio@mri.tmd.ac.jp; fax: (81)-3-5803-5829.

Published online in Wiley InterScience (www.interscience.wiley.com).

DOI 10.1002/hep.23387

Potential conflict of interest: Nothing to report.

Additional Supporting Information may be found in the online version of this article.

however, it is likely that many more factors are involved in this complex process. In particular, the mechanism underlying the local induction of liver formation remains poorly understood. This gap in our knowledge is reflected in the dearth of reports on rodent mutations that specifically interfere with the initial specification of the liver anlage.

Small fish are particularly suitable for mutational investigations because they are easy to rear in a relatively compact space, their generation times are reasonably short, and they produce transparent embryos. In many fish species, embryos develop outside the mother's body, making it easy to inspect them visually and to manipulate their tissues and cells. Our group has previously used systematic mutagenesis in medaka to generate numerous mutations affecting various aspects of liver development and function.[3-5] The focus of this paper is the recessive mutation *hiohgi* (*hio*). In wild-type (WT) medaka, the hepatic bud forms from the endoderm rod at stage 25 (50 hours post-fertilization at 27°C; 18-19 somite stage).[6] In medaka *hio* embryos, the liver does not appear until stage 29 and is small and malformed. In addition to this liver defect, *hio* mutant embryos lack pectoral fins and die after hatching. These phenotypes suggested to us that the study of *hio* mutants might allow the dissection of various aspects of embryonic specification and perhaps the linking of liver formation to fin formation.

The signaling pathway of vertebrate limb formation has been studied in detail.[7] Limbs arise from regions of the lateral plate mesoderm (LPM) at specific positions along the main anteroposterior (AP) body axis. A number of studies have shown that the limb-inducing signal originates in the axial mesoderm and is relayed from there to the LPM. In mouse, chick, and zebrafish, this signal is thought to be retinoic acid (RA), the bulk of which is synthesized by retinaldehyde dehydrogenase type2 (RALDH2) in early somites and the LPM.[8-15] With respect to downstream effectors, molecular studies have clearly shown that RA signaling from the zebrafish somitic mesoderm leads to the expression of the *wnt2ba* gene in the intermediate mesoderm, which then signals to the LPM and triggers *tbx5* expression. *Tbx5* is required for Fgf signaling in the fin bud that leads to *prdm1* expression, which in turn triggers *fgf10* and *bmp2b* expression.[7,16]

In contrast, the identity of an initial hepatic inducer in vertebrates has yet to be validated genetically. In the first report to isolate a single gene regulating vertebrate liver specification, Ober et al.[17] characterized an interesting zebrafish mutant called *prometheus* (*prt*). In *prt* embryos, the liver is absent or greatly reduced in size at 50 hours post-fertilization but may start to develop and "catch up" to normal size at a later stage. Positional cloning and further analysis revealed that the *prt* mutation altered the *wnt2bb* gene (the second *wnt2b* gene) and that *prt/wnt2bb* was expressed in restricted bilateral domains in the LPM directly adjacent to the liver-forming endoderm. Subsequently, Shin et al.[18] reported that Fgf and Bmp signaling pathways play important roles in zebrafish liver specification and raised the possibility that these molecules act downstream of Wnt2bb. However, the molecules that act upstream of Wnt2bb during liver specification remain to be identified.

In this study, we carried out a detailed characterization of our medaka *hio* mutants, whose signature phenotypes are a small liver and no pectoral fins. Our results define *hio* as a missense mutation of the *raldh2* gene, the expression of which likely results in a nonfunctional RALDH2 protein that cannot support fin development. We also show that the *hio* mutation causes a retardation of liver budding that resembles that observed in zebrafish *prt* mutants, and that *wnt2bb* expression is undetectable in *hio* LPM. Our data suggest that the role of RA signaling in the specification of both liver and fins is to induce expression of *wnt2b* family genes.

Materials and Methods

Fish Maintenance. Medaka were raised and maintained under standard laboratory conditions at approximately 27°C. Heterozygous carriers of the *hio* mutation were identified by random intercrosses. To obtain homozygous *hio* mutant embryos, heterozygous carriers of the *hio* mutation were mated. Typically, the eggs were spawned synchronously every morning. Embryos were raised at 30°C, and embryonic stages were determined based on morphological features, as previously described.[6]

Genetic Mapping. The *hio* mutation was induced in the Cab-Kyoto line of medaka.[3] The Kaga-Kyoto line of medaka was used for polymorphic marker-based genetic mapping.[3] Genetic mapping and chromosome walking were performed essentially as described.[19]

Reverse-Transcription Polymerase Chain Reaction and Gene Segment Alignment. Partial or full-length complementary DNAs of the *raldh2* (Accession number AB439727), *tbx5* (AB439834), *wnt2bb* (AB439835), *wnt2ba*, *cp*, *prox1*, *insulin*, and *tbx3* genes were generated by reverse-transcription polymerase chain reaction of messenger RNAs (mRNAs) from various stages of medaka embryos (Supporting Table 1). Alignment was performed using MultAlin (http://prodes.toulouse.inra.fr/multalin/multalin.html).

Injection of mRNA. WT *raldh2* mRNA (400 pg), obtained by *in vitro* transcription of a pBS-KS(−)-*raldh2*

clone, was injected into the cytoplasm of one-cell stage embryos that were the progeny of intercrossed *hio* heterozygotes.

Gene Knockdown by Morpholinos. Morpholino oligonucleotides (MOs) were synthesized by Gene-Tools, LLC (Corvallis, OR). MOs (0.8 pmol) were injected into the cytoplasm of one-cell stage WT medaka embryos. The sequences of MOs used were as follows:

raldh2 MO, 5′-ATGACTGCCGTGGCTGCGCTGCTGT-3′;

wnt2bb MO, 5′-ATATACCTGAGAGTGTCCAGAACAG-3′.

Retinoic Acid Treatments. Embryos resulting from *hio* heterozygote intercrosses were incubated in the dark from stage 21 onward in various dilutions of a 10^{-2} M all-*trans* RA (Sigma) stock solution in dimethylsulfoxide. The diluent was 1× balanced salt solution composed of 110 mM NaCl, 5 mM KCl, 1 mM $CaCl_2$, and 2.2 mM $MgSO_4$, pH7.5. Teratogenic effects (such as disrupted heart and AP axis) were observed at 10^{-8} M all-*trans* RA and above.

Whole-Mount* In Situ *Hybridization. Whole-mount *in situ* hybridization was performed as previously described,[3] using antisense DIG-labeled riboprobes generated from medaka *tbx5*, *wnt2ba*, *prox1*, *cp*, *insulin*, *wnt2bb*, *tbx3*, or *raldh2* partial or full-length complementary DNAs. Probes used to detect *gata6*, *foxA3*, *ck19*, and *pdx1* expression were as previously described.[4]

N-([6-(2,4-Dinitro-Phenyl) Amino] Hexanoyl)-1-Palmitoyl-2-BODIPY-FL-Pentanoyl-sn-Glycero-3-Phosphoethanolamine–Mediated Tracking of Lipid Metabolism. Medaka embryos at stage 36 were placed in 0.5 mL 1× balanced salt solution containing 0.3 mg/mL N-([6-(2,4-dinitro-phenyl)amino]hexanoyl)-1-palmitoyl-2-BODIPY-FL-pentanoyl-*sn*-glycero-3-phosphoethanolamine (PED6) and incubated in the dark for 4 hours at 28°C. The treated embryos were rinsed with 1× balanced salt solution and placed in a glass depression slide. PED6 fluorescence was detected using a Zeiss Axioplan 2 microscope.

Results

The* hio *Mutation Alters the* raldh2 *Gene. Using bulked segregation analysis, we performed positional cloning and mapped hio between restriction fragment length polymorphisms OLc2806f and Scaf21_1.0M on LG3 (Fig. 1A). This region includes a sequence with homology to the mammalian and zebrafish *raldh2* genes. Because the "missing fin" phenotype of medaka *hio* mutants was similar to that of the zebrafish *raldh2* mutants *neckless* (*nls*) and *no-fin* (*nof*),[8,10] *raldh2* appeared to be a good candidate for the gene affected by the *hio* mutation. We compared the sequence of a genomic fragment encoding the WT medaka *raldh2* gene with the sequences of the corresponding fragments from four independent homozygous *hio* embryos. We found an A to G transversion in *hio* alleles that would cause the threonine 468 residue in the WT RALDH2 enzyme to be replaced by alanine (Fig. 1B). A comparison of the predicted WT RALDH2 amino acid sequences among medaka, human, xenopus, and zebrafish revealed an overall amino acid sequence identity of 81% (between medaka and human or xenopus) and 84% (between medaka and zebrafish) (Fig. 1C). The threonine 468 residue was conserved among all species examined. Moreover, threonine 468 lies within the catalytic domain of WT RALDH2 (Fig. 1C). These results suggest that the mutant RALDH2 protein produced in *hio* mutants is inactive.

It has been well established that the defects of RA signaling lead to the impairment of fin development in zebrafish.[7,8,10,16] We showed that the injection of *RALDH2*-MO into WT embryos results in the impairment of fin development, and the injection of *raldh2* mRNA or exogenous RA rescued the defects of fin development of *hio* mutant (Supporting Fig. 1). These results indicate that RALDH2 and RA regulate fin development in medaka. In addition, *hio* embryos lacked *tbx5* and *wnt2ba* expression, which acted downstream of RA during fin development (Supporting Fig. 2). Taken together, we concluded that RA signaling plays important roles in fin development in medaka.

Loss-of-Function of RALDH2 Reduces Liver Size in Medaka. We have previously reported that the medaka *hio* mutation results in a small and malformed liver.[3] To examine the role of *raldh2*-dependent signaling in liver formation in medaka, we employed three approaches. First, to investigate whether loss-of-function of *raldh2* could account for this liver defect, we injected *raldh2*-MO into WT embryos and inspected the developing liver. We found that the *raldh2* morphants had the same undersized livers as the *hio* mutants (Fig. 2A). Estimation of liver size via *in situ* hybridization using a *gata6* probe confirmed the reduced liver size in the *raldh2* morphants (Fig. 2B). Second, to determine whether the *hio*/*raldh2* mutation was responsible for the small livers of these mutants, we injected *in vitro* transcribed *raldh2* mRNA into the cytoplasm of one-cell stage embryos that were the progeny of intercrossed *hio* heterozygotes and used *gata6 in situ* hybridization to assay these embryos for rescue of liver size. As expected, 25% of the progeny of intercrossed *hio* heterozygotes (uninjected controls) had small livers. In contrast, the percentage of progeny with

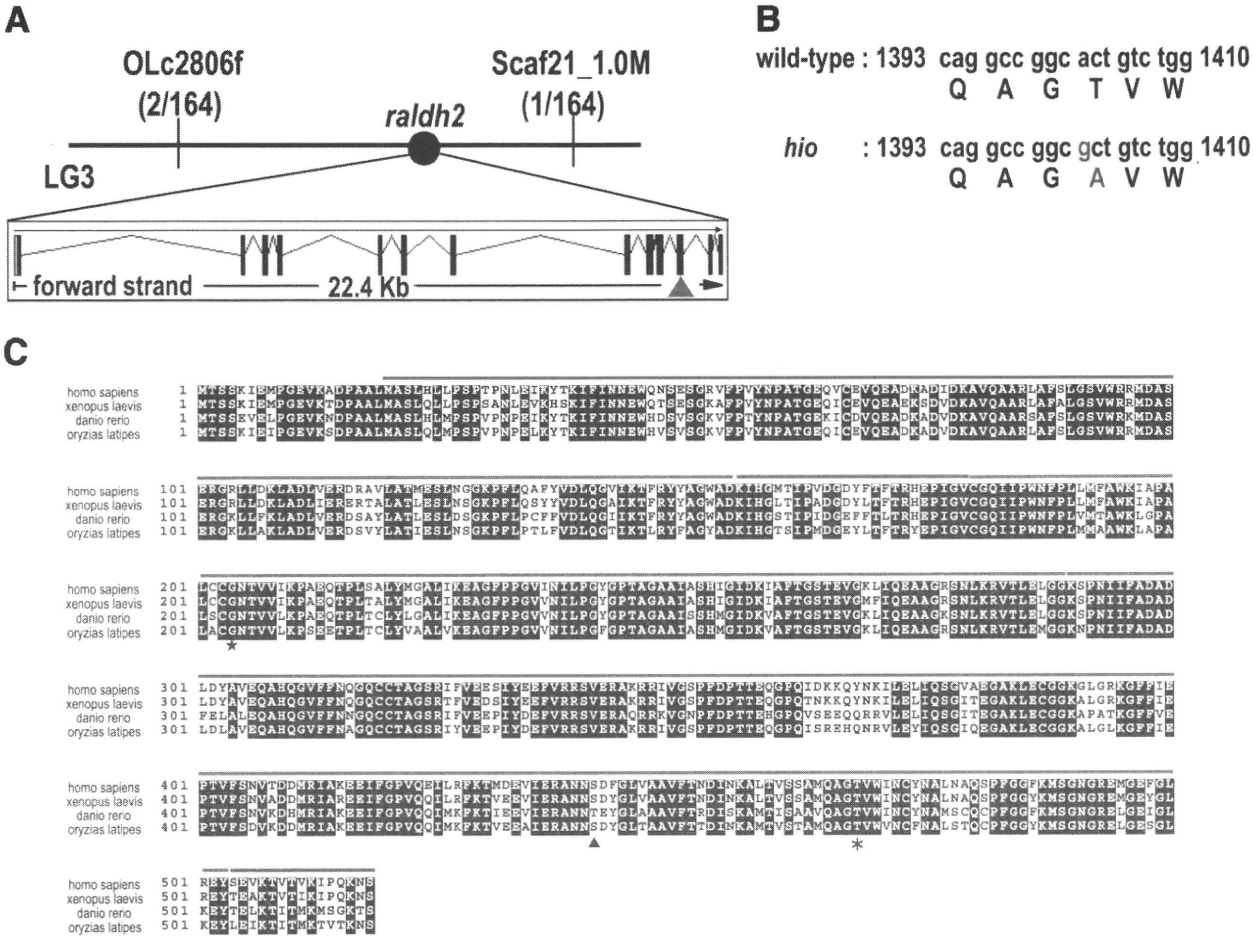

Fig. 1. Mapping and cloning of medaka *hio/raldh2*. (A) Genetic map of the locus affected by the *hio* mutation and the exon/intron structure of the medaka *raldh2* gene. The position of the *hio* mutation is indicated by the red triangle. (B) Comparison of the medaka WT *raldh2* and *hio* nucleotide sequences (lower case) and the corresponding deduced RALDH2 amino acid sequences (upper case). The *hio* mutation and the amino acid it affects are shown in red. (C) Alignment of the deduced amino acid sequences of RALDH2 proteins in *Homo sapiens* (Accession number BAA34785), *Xenopus laevis* (AAG32057), *Danio rerio* (zebrafish; AAL00899), and *Oryzias latipes* (medaka; AB439727). Residues on a black background are conserved among all four species. Red, green, and blue horizontal lines indicate the RALDH2 catalytic domain (289-503), nucleotide binding domain (20-154, 179-288), and tetramerization domain (155-178, 504-518), respectively.[29] The asterisk indicates the position of the *hio* mutation (T468A) in medaka. The star and triangle indicate the positions of the zebrafish *nls* (G204R) and *nof* (T441K) mutations, respectively.

decreased liver size was reduced to 14% after injection of *raldh2* mRNA (Fig. 2C). Finally, we investigated whether treatment with exogenous RA, the bulk of which is synthesized by RALDH2, could rescue the liver defects caused by the *hio* mutation. We treated the progeny of intercrossed *hio* heterozygotes with all-*trans* retinoic acid (atRA) and monitored liver development. Whereas 25% of the untreated progeny of intercrossed *hio* heterozygotes had small livers, the percentage of progeny with a small liver was reduced to 13% after exposure to 5×10^{-9} M atRA (Fig. 2D). Thus, treatment with either WT *raldh2* mRNA or exogenous RA can rescue the small liver phenotype in at least some *hio* mutants, although the efficiency of such rescue is much lower for the liver than for the pectoral fin. When the livers of *hio* mutants with treatment with either WT *raldh2* mRNA or exogenous RA became as large as that of WT medaka, we judged it to be rescued. Therefore, we may have underestimated the recovery rate of liver phenotype. In any case, the loss of *raldh2* function in *hio* mutants causes a defect not only in pectoral fin development but also in liver formation.

The* hio *Mutation Retards Liver Specification. Although the molecular mechanism by which RA signaling initiates fin development is well established,[7,20] the molecular regulation of liver development by RA signaling remains to be elucidated. To address this issue, we used *in situ* hybridization with a probe specific for the endodermal marker *foxA3* to monitor liver development in *hio* embryos. Whereas hepatic buds were observed in WT medaka at stage 25, these structures did not form in *hio* mutants until stage 29 (Fig. 3A). By stage 32, hepatic buds were noticeably smaller in *hio* embryos compared

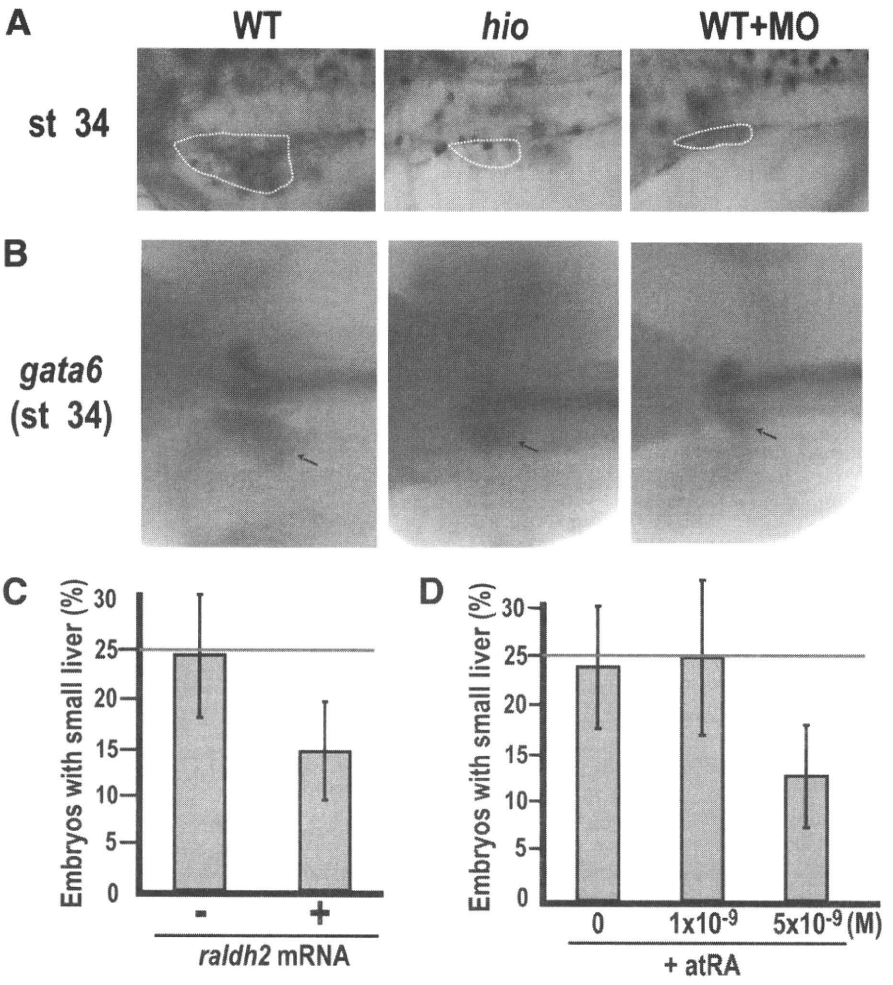

Fig. 2. Impaired liver formation in *hio* embryos is attributable to loss of *raldh2* function. (A) Lateral views of WT, *hio* mutant, and *raldh2* morphant (MO) embryos at stage 34. Dotted lines highlight the liver region. (B) Whole-mount *in situ* hybridization to detect *gata6* expression in WT, *hio* mutant, and *raldh2* morphant (MO) embryos at stage 34. Arrows indicate the liver region. For A-C, images shown are one example representative of more than 10 embryos examined per group. (C) Rescue of the *hio* mutation by *raldh2* mRNA. Progeny one-cell embryos of intercrossed *hio* heterozygotes were injected with *raldh2* mRNA (n = 49), and liver development was monitored. In the absence of *raldh2* mRNA (n = 50), the expected 25% (red line) of progeny (*hio* homozygotes) showed impaired liver development. Bars indicate the mean ± standard error. (D) Rescue of the *hio* mutation by all-*trans* retinoic acid (atRA) treatment. Progeny one-cell embryos of intercrossed *hio* heterozygotes were treated with the indicated concentrations of atRA (0 M; n = 50, 1×10^{-9} M; n = 32, 5×10^{-9} M; n = 39), and liver development was monitored. In the absence of 5×10^{-9} M atRA, the expected 25% (red line) of progeny (*hio* homozygotes) showed impaired liver development. Bars indicate the mean ± standard error.

with the WT. These data indicate that the medaka *hio* mutation retards hepatic bud formation.

Next, we determined whether the *hio* mutation interferes with the initial specification of liver anlage in medaka. We carried out *in situ* hybridization using a probe for the hepatic specification marker *prox1* to monitor liver specification. In WT medaka embryos, *prox1* was induced in the hepatic bud starting at stage 25 (Fig. 3B, upper panel), and by stage 29, *prox1*-positive cells were observed only in the hepatic region. In *hio* embryos, the formation of the hepatic bud was delayed until stage 29 (Fig. 3A), so that *prox1*-positive cells were not observed in the hepatic region until this stage (Fig. 3B, bottom panel). These results indicate that the *hio* mutation compromises the signaling pathway required for initial hepatic fate specification.

The Small Livers in* hio *Embryos Exhibit Normal Hepatic Cell Differentiation and Function. The most important cell types in the vertebrate liver are cholangiocytes (bile duct cells) and hepatocytes. To determine whether hio livers were capable of normal hepatic cell differentiation, we subjected WT and *hio* embryos to *in situ* hybridization with a probe for the cholangiocyte marker *cytokeratin19* (*ck19*) and the hepatocyte marker *ceruloplasmin* (*cp*). At stage 28, although WT embryos showed a few *ck19*-positive cells in the hepatic region, *hio* embryos did not (Supporting Fig. 3). However, by stage 32, *ck19* expression was comparable in WT and *hio* livers (Fig. 4A, left panel). Furthermore, *cp* expression was comparable in WT and *hio* livers at stage 34 (Fig. 4A, right panel). Thus, although liver formation is delayed in *hio* embryos, the small livers of these mutants can give rise to differentiated liver cells. To ascertain whether the small *hio* liver was functional, we took advantage of a reporter system based on PED6, a fluorescent phospholipid.[21] When WT medaka ingest PED6, endogenous lipase activity and the rapid transport of cleavage products results in intense gallbladder fluorescence.[4] We observed equivalent levels of green fluorescence in the gallbladders of WT and *hio* embryos treated with PED6 at stage 36 (Fig. 4B), indicating that *hio* livers have a normal capacity to metabolize lipids. Taken together, our results show that loss of *raldh2* function initially impairs liver specification and retards liver development but does not impair hepatic